Synthesis and biological evaluation of new epalrestat analogues as aldose reductase inhibitors (ARIs)

ARTICLE *in* EUROPEAN JOURNAL OF MEDICINAL CHEMISTRY · NOVEMBER 2013

Impact Factor: 3.45 · DOI: 10.1016/j.ejmech.2013.10.043 · Source: PubMed

9 AUTHORS, INCLUDING:

Ravinder Mettu
Academia Sinica
17 PUBLICATIONS **226** CITATIONS
SEE PROFILE

Pankaj K. Bagul
Translational Health Science and Technolo…
12 PUBLICATIONS **117** CITATIONS
SEE PROFILE

Chandrakant Deoram Bagul
National Institute for Pharmaceutical Educ…
17 PUBLICATIONS **48** CITATIONS
SEE PROFILE

Sanjay K Banerjee
Translational Health Science and Technolo…
44 PUBLICATIONS **1,151** CITATIONS
SEE PROFILE

European Journal of Medicinal Chemistry 71 (2014) 53–66

Contents lists available at ScienceDirect

European Journal of Medicinal Chemistry

journal homepage: http://www.elsevier.com/locate/ejmech

Original article

Synthesis and biological evaluation of new epalrestat analogues as aldose reductase inhibitors (ARIs)

Thatikonda Narendar Reddy [a], Mettu Ravinder [a], Pankaj Bagul [b], Keerthi Ravikanti [b], Chandrakant Bagul [c], Jagadeesh Babu Nanubolu [d,**], Kolupula Srinivas [c,**], Sanjay K. Banerjee [b,**], Vaidya Jayathirtha Rao [a,c,*]

[a] Crop Protection Chemicals Division, CSIR-Indian Institute of Chemical Technology, Hyderabad 500607, India
[b] Division of Medicinal Chemistry and Pharmacology, CSIR-Indian Institute of Chemical Technology, Hyderabad 500607, India
[c] Department of Medicinal Chemistry, National Institute of Pharmaceutical Education & Research, Balanagar, Hyderabad 500037, India
[d] Centre for X-ray Crystallography, CSIR-Indian Institute of Chemical Technology, Hyderabad 500607, India

ARTICLE INFO

Article history:
Received 1 July 2013
Received in revised form
26 September 2013
Accepted 13 October 2013
Available online 6 November 2013

Keywords:
Baylis–Hillman reaction
Rhodanine compounds
Epalrestat analogues
Crystal structure
Molecular docking
Aldose reductase inhibitors

ABSTRACT

Baylis–Hillman chemistry derived four series of new epalrestat analogues were synthesized. Three structural changes are introduced in these 39 new epalrestat analogues synthesized. All compounds were evaluated for their *in vitro* aldose reductase inhibitory (ALR) activity. Biological activity data indicates that compounds **6**, **16**, **19**, **28** and **29** are potent and the activity is in the range of reference drug, epalrestat. Molecular modelling studies were performed to understand the binding interactions of these active molecules with the ALR protein. Molecular docking data indicates the key interactions of epalrestat were retained in some of the active compounds whereas some new interactions were noticed for other molecules. The modifications introduced on epalrestat have impact for developing a new-type of ALR inhibitor.

1. Introduction

Type 2 Diabetes mellitus, also known as non-insulin dependent diabetes mellitus (NIDDM) is a type of metabolic disease in which the body loses its ability to control glucose levels in normal range. This is because of either from the alteration of insulin secretion by pancreas or development of insulin resistant by different organs especially skeletal muscle [1]. This disease is recognized as a chronic disease with high morbidity and mortality, and poses an economic burden for developing countries [2]. A recent study by WHO reveals that there were approximately 200 million people globally, ranging age 20–80 years, suffering from diabetes and this figure expected to increase to 366 million by the year 2030 [3]. Diabetic patients on prolonged exposure to uncontrolled hyperglycemia lead to several diabetic complications [4] such as retinopathy [5], neuropathy [6], cataracts [7], nephropathy [8] and cardiovascular complication [9].

Activation of several biochemical pathways has been proposed by researchers, to explain the mechanism of diabetic complications [10]. Among these, polyol pathway is the most promising one and has been studied extensively [11]. Activation of polyol pathway has been reported in diabetic condition. Aldose reductase (ALR), the first and rate limiting enzyme of the polyol pathway is responsible for the conversion of glucose into sorbitol (Fig. 1) [12]. Generally, under euglycemia condition, most of the glucose metabolized to pyruvate *via* glycolytic pathway and very less amount of the glucose metabolized through polyol pathway. Therefore the role of the polyol pathway in glucose metabolism is very minor. However, when glucose levels are elevated, the contribution of the polyol pathway significantly increases, and that results in accumulation of sorbitol in the cells [13]. As a result, both oxidative stress and osmotic stress increases in the cells and leads to cellular damage that contribute to diabetic complications [14]. Although several oral hypoglycemics available in the market, but they are not that effective [15]. The achievement and maintenance of euglycemia is extremely difficult for the people with advanced stages of diabetes.

* Corresponding author. Crop Protection Chemicals Division, CSIR-Indian Institute of Chemical Technology, Hyderabad 500607, India.
** Corresponding authors.
E-mail addresses: jrao@iict.res.in, jayathirtha.vaidya@rediffmail.com (V.J. Rao).

0223-5234/$ – see front matter © 2013 Elsevier Masson SAS. All rights reserved.
http://dx.doi.org/10.1016/j.ejmech.2013.10.043

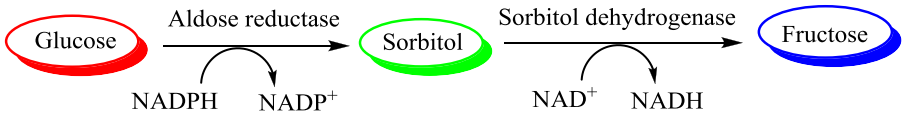

Fig. 1. Schematic diagram for polyol pathway.

However, the quality of life of diabetic patients can be improved by preventing diabetic associated complications and this can be achieved by the inhibition of aldose reductase (ALR) enzyme. Hence, there is a need to synthesize new molecules that can substantially delay or prevent the development of diabetic complications through inhibition of ALR enzyme [16].

Recently, ARIs has become an attractive therapeutic strategy [17] and a variety of ARIs with different pharmacophore group have been synthesized and tested for their efficacy in several diabetic complications by researchers over the last two decades (Fig. 2). Based on their chemical structure, they can be classified into three general groups: (i) carboxylic acid derivatives (such as Zopolrestat, Epalrestat, Zenarestat, Ponalrestat, Tolrestat and recently developed Lidorestat); (ii) spirohydantoins (includes Sorbinil, Ranirestat, AND-138 and Fidarestat); (iii) flavonoids (such as Quercetin and Resveratrol). But most of them were failed at clinical trials because of their side effects or poor efficacy [18]. Epalrestat is the only approved drug and it is currently used for the treatment of diabetic neuropathy in Japan, China and recently in India [19].

During the past ten years, a great deal of our efforts has been devoted to Baylis–Hillman chemistry [20] and its applications towards the synthesis of new heterocyclic compounds along with their potential biological activities [21]. In the present study we describe the synthesis of new epalrestat analogues using Baylis–Hillman chemistry together with their aldose reductase inhibitor activity. Furthermore, we have performed molecular modelling studies for selected compounds to study the interaction with ALR enzyme from molecular prospective.

2. Results and discussion

2.1. Chemistry

In view of the fact, that the rhodanine (thiazolidine) functionality is essential for ARI activity (Fig. 2, epalrestat), we focused on the synthesis of new epalrestat analogues carrying other functional groups. In this context, to increase the efficacy of epalrestat we mainly modified epalrestat in three domains: (i) substituted phenyl, furyl, thienyl or naphthyl ring in place of phenyl ring, (ii) nitrile group in place of methyl, and (iii) kept the rhodanine moiety intact but sometimes replaced the acetic acid group by benzoic acid, phenyl acetic acid and hydrogen moieties for the study (Fig. 3). The stereochemistry of two double bonds kept intact.

A series of new epalrestat analogues were synthesized as outlined in Scheme 1 and Table 1. Aromatic aldehydes (**2a**–**2l**) with suitable substitution were reacted with acrylonitrile (**3**) in the presence of catalyst DABCO, under solvent free conditions [22] leading to the formation of Baylis–Hillman adducts (**4a**–**4l**). The Baylis–Hillman adducts (**4a**–**4l**) were oxidized using ionic liquid [23a] [Hmim] HSO_4 and $NaNO_3$ to obtain corresponding [E]-α-cyanocinnamaldehyde derivatives (**5a**–**5l**) with control of double bond stereochemistry [23]. The [*E*]-α-cyanocinnamaldehyde derivatives (**5a**–**5l**) were treated with rhodanine compounds under Knoevenagel condensation conditions to obtain final compounds (**6**–**44**) with control of double bond stereochemistry [24]. Rhodanine compounds **1a** and **1b** (Fig. 4) were obtained commercially whereas **1c** and **1d** (Fig. 4) were prepared as per the published procedure [25]. X-ray crystal structure is determined for compound **39**, which helped us in further defining stereochemistry of two double bonds (Fig. 5). The new epalrestat analogues synthesized are grouped in to four series (Scheme 1, Table 1 and Chart 1).

Accordingly, we first examined the aldehyde (**5a**) with the rhodanine acetic acid (**1a**) as a choice of substrates for the study using various organic and inorganic bases under different solvent systems (Table 2). After many trials, we finally settled with an efficient procedure for the synthesis of epalrestat analogues (**6a**) in good yield (81%), when the reaction was carried out in acetic acid as a solvent and NH_4OAc as a base (Table 2). Encouraged by this successful result, we examined all other aldehydes with various rhodanine compounds (**1a**–**1d**) and the results are summarized in Table 1.

2.2. Biological activity

2.2.1. Aldose reductase inhibitory activity

Thus synthesized 39 epalrestat analogues were taken forward to understand their ability towards aldose reductase inhibition. The enzyme aldose reductase converts aldehydes to alcohols in the presence of NADPH. Based on this property of aldose reductase, we used a kinetic based assay for the evaluation of inhibition of aldose reductase activity with the synthesized compounds (**6**–**44**). For this assay we used DL-glyceraldehyde as an aldehyde which is reduced to glycerol, in the presence of NADPH by aldose reductase enzyme. NADPH is a cofactor that is being oxidized to $NADP^+$. Therefore we measured the absorbance of unchanged NADPH, at different time intervals and at 340 nm. Absorbances of respective blanks were taken before adding NADPH [31].

All the synthesized compounds **6**–**44** were evaluated *in vitro* for their ability to inhibit aldose reductase activity using epalrestat as reference compound and results are presented in Fig. 6. Among the all 39 compounds, **6**, **16**, **19**, **28** and **29** exhibited more than 50% inhibition and were comparable to standard drug epalrestat while the rest of the compounds exhibited less than 50% inhibition. The IC_{50} values were determined for those compounds displaying greater than 50% inhibition and corresponding data presented in Table 3 and Fig. 7. Among the all tested compounds, **29** found to be the most potent aldose reductase inhibitor with an IC_{50} value of 0.22 μM compared to the standard, epalrestat which has IC_{50} value 0.4 μM. Other compounds **6**, **16**, **19** and **28** exhibited excellent inhibitory activities with IC_{50} values of 0.75, 0.67, 0.69 and 0.86 μM respectively.

The 39 analogue compounds synthesized were grouped as series 1 to 4 (Chart 1, Table 1). Under the series 1 (compound **6**–**17**, Chart 1, Table 1) compound **6** and **16** are found to be comparable with standard epalrestat (Table 3) and the remaining compounds **7**–**15** and **17** are moderately active. Considering the epalrestat structure, the methyl group is replaced by an electron withdrawing nitrile group on the olefin chain did not make much difference in compound **6**, in terms of its activity. The phenyl group having various substitutions (**7**–**13**, Chart 1, Table 1) did reflect in lowering inhibition activity. Replacing the phenyl group by naphthyl (compound **14**) or with thiophene (compound **17**) also provided reduced ARI activity. Compound **16** has furan ring and exhibited excellent activity comparable with epalrestat. All these compounds **6**–**17** carry rhodanine acetic acid end group as epalrestat. Compounds in series 2 (**18**–**28**, Chart 1, Table 1) carry three changes introduced.

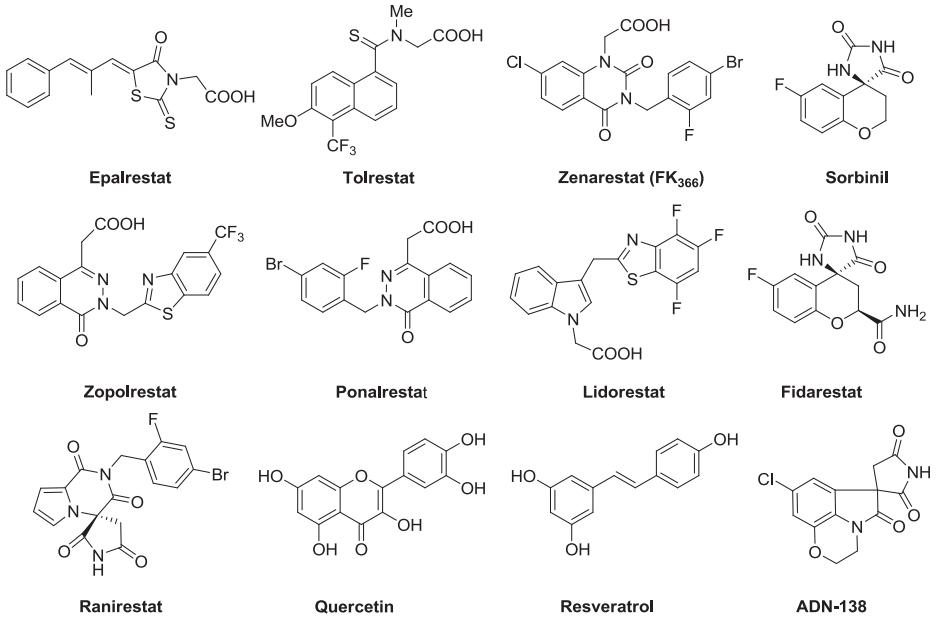

Fig. 2. Chemical structures of some known aldose reductase inhibitors (ARIs).

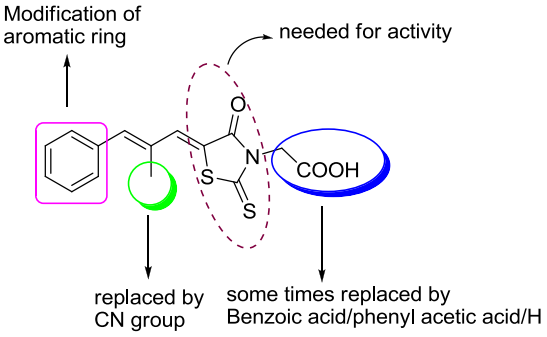

Fig. 3. Structural modification of epalrestat.

The methyl group on the olefin chain is replaced by nitrile, did not make much difference. The rhodanine acetic acid is replaced by just rhodanine, not carrying acetic acid end group did reflected that, it is not mandatory in exerting ARI activity as evidenced in compounds **19** and **28**. The compounds given in Fig. 2, quercetin (phenolic hydroxy), sorbinil, and ADN-138 are ARIs and do not carry carboxylic group. Further the compound **19** has a substituent at the *para* position of phenyl group. The compound **28** indicates that replacing the phenyl group by thiophene residue did not affect much in the ARI activity. The observation made in the compounds of series 2 (**18**–**28**, Chart 1, Table 1) not carrying acetic acid end group, but still exerting the ARI activity (compound **19** and **28**) is new and interesting in terms of understanding the small molecules and macromolecular interactions leading to its functioning. Series 3

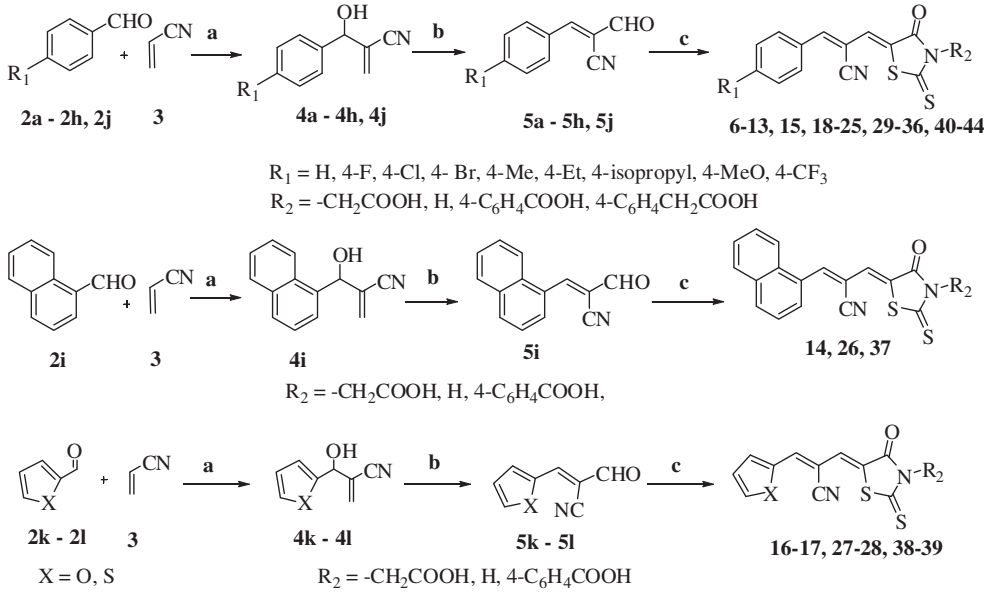

Scheme 1. Synthesis of epalrestat analogues. *Reagents and conditions*: (a) DABCO (30 mol %), overnight; (b) [Hmim] HSO_4, $NaNO_3$, 80 °C; (c) **1a**–**1d**, NH_4OAc, AcOH, reflux.

Table 1
Synthesis of rhodanine derivatives from cyanocinnamaldehyde.

S. no	Aldehyde	Rhodanine	Product	Yield (%)
1	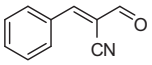 **5a**	**1a**	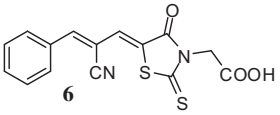 **6**	81
2	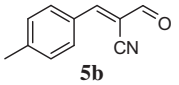 **5b**	**1a**	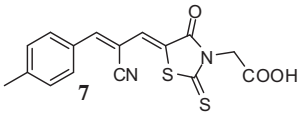 **7**	83
3	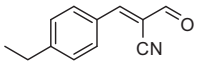 **5c**	**1a**	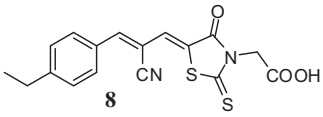 **8**	80
4	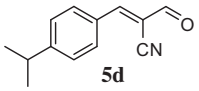 **5d**	**1a**	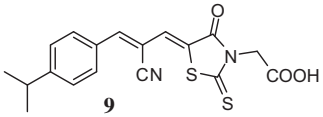 **9**	82
5	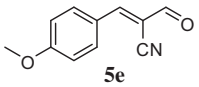 **5e**	**1a**	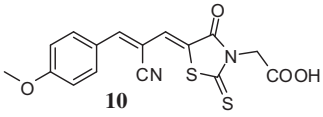 **10**	68
6	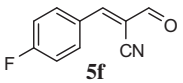 **5f**	**1a**	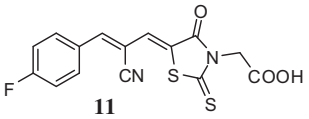 **11**	74
7	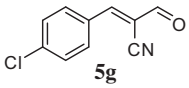 **5g**	**1a**	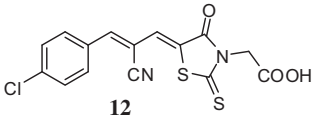 **12**	72
8	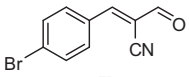 **5h**	**1a**	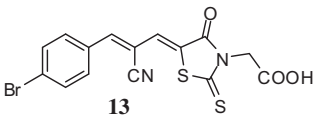 **13**	73
9	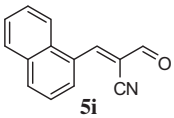 **5i**	**1a**	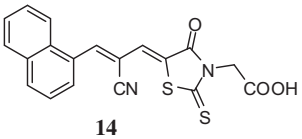 **14**	75
10	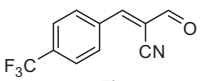 **5j**	**1a**	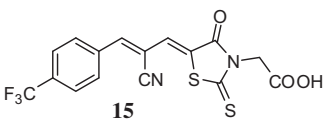 **15**	72
11	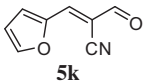 **5k**	**1a**	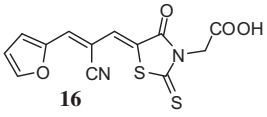 **16**	79
12	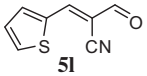 **5l**	**1a**	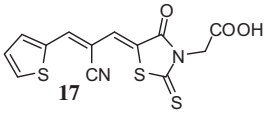 **17**	80

Table 1 (*continued*)

S. no	Aldehyde	Rhodanine	Product	Yield (%)
13	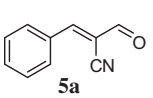 **5a**	**1b**	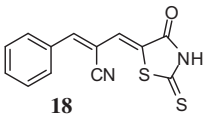 **18**	68
14	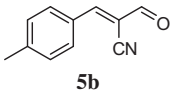 **5b**	**1b**	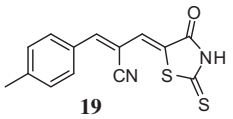 **19**	70
15	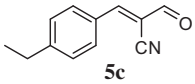 **5c**	**1b**	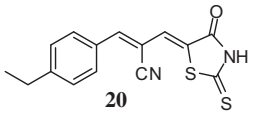 **20**	73
16	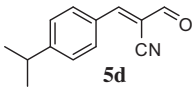 **5d**	**1b**	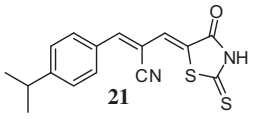 **21**	73
17	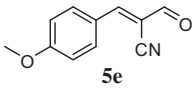 **5e**	**1b**	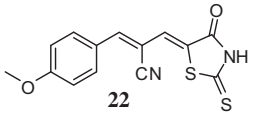 **22**	69
18	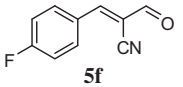 **5f**	**1b**	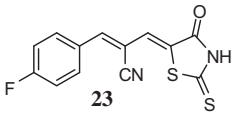 **23**	68
19	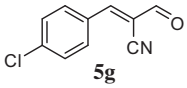 **5g**	**1b**	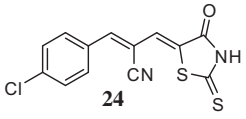 **24**	65
20	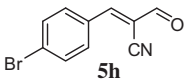 **5h**	**1b**	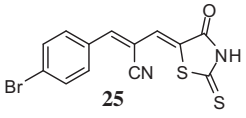 **25**	65
21	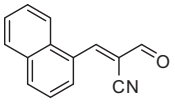 **5i**	**1b**	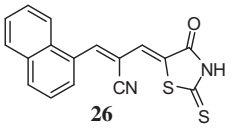 **26**	73
22	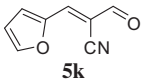 **5k**	**1b**	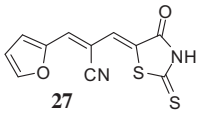 **27**	80
23	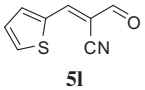 **5l**	**1b**	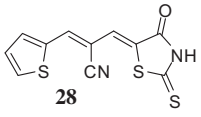 **28**	81
24	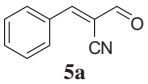 **5a**	**1c**	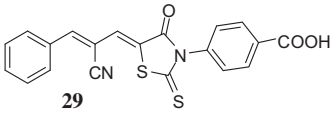 **29**	65

(*continued on next page*)

Table 1 (*continued*)

S. no	Aldehyde	Rhodanine	Product	Yield (%)
25	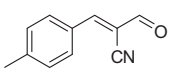 **5b**	**1c**	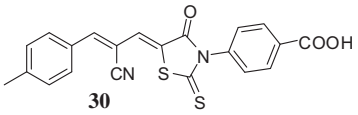 **30**	70
26	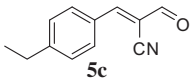 **5c**	**1c**	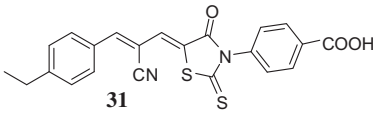 **31**	68
27	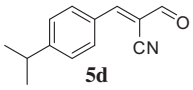 **5d**	**1c**	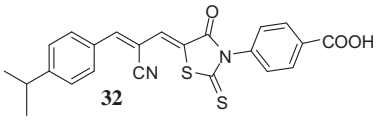 **32**	69
28	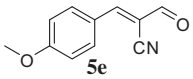 **5e**	**1c**	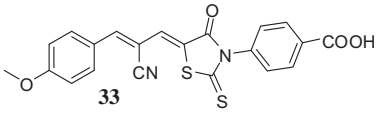 **33**	65
29	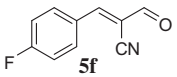 **5f**	**1c**	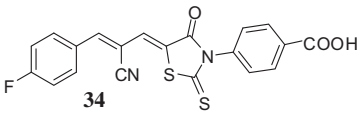 **34**	62
30	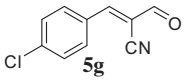 **5g**	**1c**	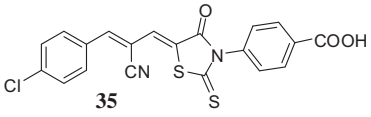 **35**	65
31	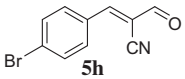 **5h**	**1c**	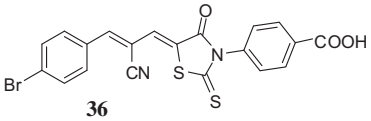 **36**	62
32	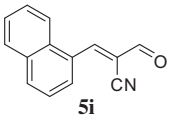 **5i**	**1c**	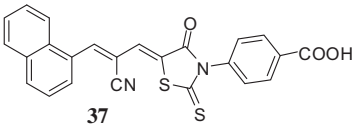 **37**	72
33	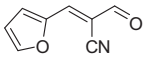 **5k**	**1c**	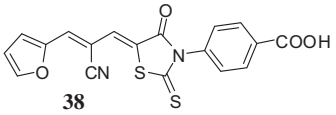 **38**	79
34	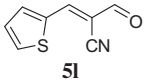 **5l**	**1c**	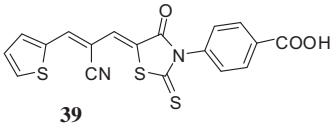 **39**	79
35	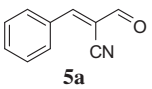 **5a**	**1d**	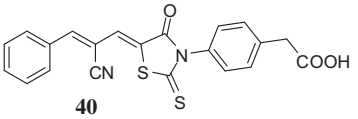 **40**	72
36	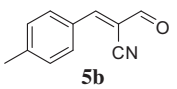 **5b**	**1d**	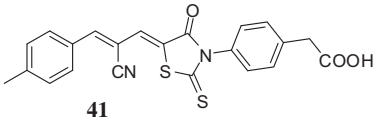 **41**	75

Table 1 (*continued*)

S. no	Aldehyde	Rhodanine	Product	Yield (%)
37	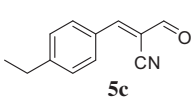 **5c**	**1d**	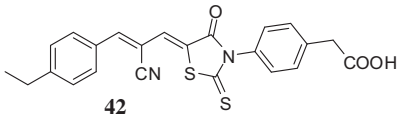 **42**	78
38	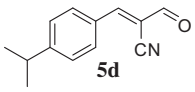 **5d**	**1d**	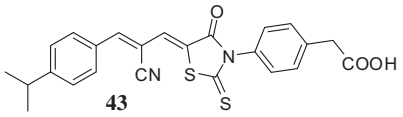 **43**	79
39	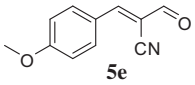 **5e**	**1d**	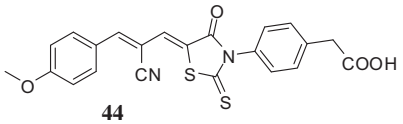 **44**	75

compounds (**29**–**39**) have the special feature of replacing acetic acid by benzoic acid. Out of 11 compounds of series 3, only one compound **29** showed excellent activity. This is also an interesting observation that benzoic acid end group can also exert excellent ARI activity. The compounds of series 4, **40**–**44** (Chart 1, Table 1) carrying phenyl acetic acid end group did not contribute to ARI activity and all these five compounds **40**–**44** are moderately active compare to epalrestat standard. The structural changes introduced

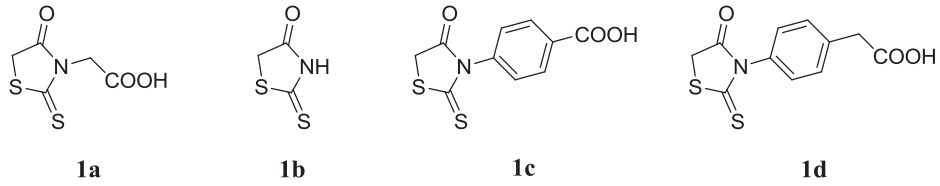

1a **1b** **1c** **1d**

Fig. 4. Various rhodanine compounds used to make new ARIs.

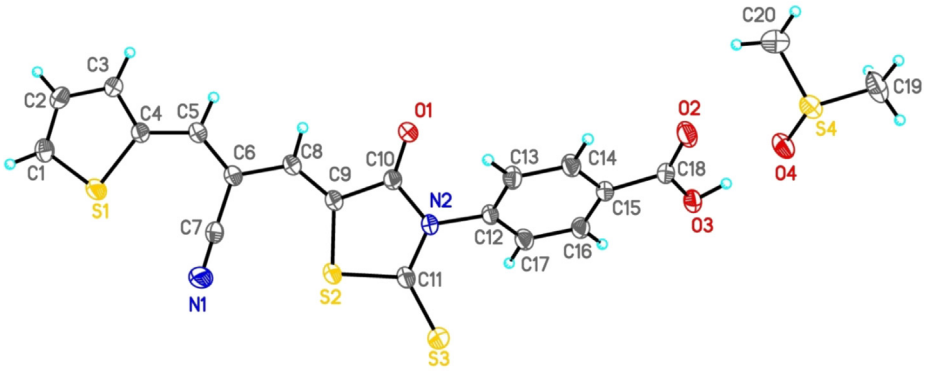

Fig. 5. The molecular structure of 39 with the atom-numbering scheme. Displacement ellipsoids are drawn at 30% probability level and H atoms are shown as small spheres of arbitrary radius. The molecule crystallizes with DMSO solvent in 1:1 stoichiometric ratio.

Series 1: 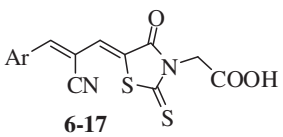 **6-17**

Series 2: 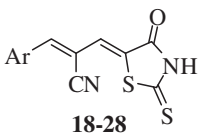 **18-28**

Series 3: 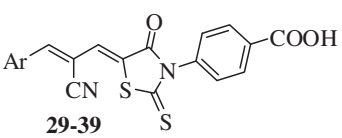 **29-39**

Series 4: 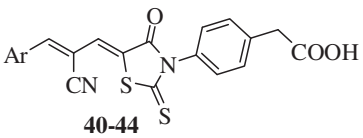 **40-44**

Chart 1. Classification of 39 compounds in to four series.

Table 2
Effect of different bases and solvents on the reaction of compound **5a** with **1a**.

S. no.	Base (1 equiv.)	Solvent	Yield (%)
1	Piperidine	Ethanol (reflux)	70
2	K_2CO_3	DMF (110 °C)	30
3	NH_4OAc	Toluene (110 °C)	55
4	NH_4OAc	DMF (110 °C)	35
5	NH_4OAc	CH_3COOH (110 °C)	81
6	NaOAc	CH_3COOH (110 °C)	75

in making 39 epalrestat analogues revealed new and interesting structure activity relationships.

2.2.2. Docking

In order to gain insight about protein–ligand interactions of newly synthesized analogues in the active site of aldose reductase enzyme, molecular docking study was performed. The aldose reductase enzyme complexed with tolrestat (PDB ID: 2FZD) was selected [26]. Geometries of five active molecules were optimized by PM3 method using Gaussian 09 software [27]. The docking simulations in the active site of aldose reductase enzyme were done with aid of FlexX software [28] as it was observed the reproduction of binding interactions (Y48, H110, W111) of co-crystal with enzyme when tolrestat is docked into the active site of it. All the active compounds (**6**, **16**, **19**, **28** and **29**) along with epalrestat (reference compound) were docked into the same active site of tolrestat (2FZD) and the results are summarized in Table 4. Among the five active compounds, compound **6**, **16** and **29** were exhibited same interactions (Y48, H110, W111) as co-crystal ligand in anionic site and within these series, compound **16** and **29** exhibited additional interactions with S302 (Fig. 8). The binding poses of these compounds are same as epalrestat in the anionic site of the enzyme. The common feature in these molecules is the presence of carboxylic acid functional group at the rhodanine terminal. Unlike epalrestat, compounds **19** and **28** adopted different poses and exhibited interactions with other residues of enzyme (Table 4). Both these compounds possess the free amide group in rhodanine.

3. Conclusion

In this paper we described the synthesis, biological activity, and structure–activity relationships of a series of epalrestat analogues. Baylis–Hillman adducts were used in the synthesis of these newer epalrestat analogues. These are four series of compounds with free amide, *N*-acetic acid, *N*-benzoic acid and *N*-phenyl acetic acid. X-ray crystal structure helped us to define the stereochemistry of two double bonds. Compounds **6**, **16**, **19**, **28** and **29** found to be active and the IC_{50} values of these compounds are in the same magnitude

Table 3
Aldose reductase inhibitory activity (IC_{50}) of new epalrestat analogues.

Comp. no	IC_{50} (μM)
6	0.75
16	0.67
19	0.69
28	0.86
29	0.22
Epalrestat	0.40
Epalrestat [29]	0.87
Epalrestat [30]	0.10

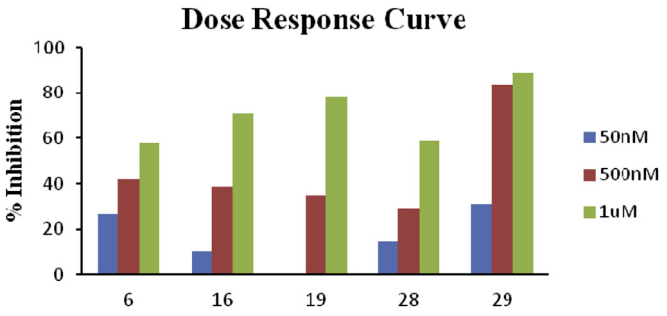

Fig. 7. Concentration dependent aldose reductase inhibitory activity of most active new epalrestat analogues.

of the reference compound, epalrestat. Molecular docking studies gave an idea about the binding of these inhibitors, which in turn helped us to understand the role of acetic acid group. The present study demonstrated structural modification on epalrestat and showed five hit compounds from four series of compounds. These results of these bindings help us to design newer molecules/analogues towards developing potent ALR inhibitors.

4. Experimental section

4.1. Chemistry

General: All commercially available chemicals were used without further purification. Melting points were determined on a Mel-Temp apparatus and are uncorrected. IR spectra were recorded using a Thermo Nicolet Nexus 670 FTIR spectrometer. The NMR spectra were recorded on Brucker Avance 300 magnetic resonance spectrometer at 300 MHz for ^1H and 75 MHz for ^{13}C respectively, using TMS as internal standard. The chemical shifts are expressed as δ values in parts per million (ppm) and the coupling constants (J) are given in hertz (Hz). ESI-MS was obtained on Thermo-Finnigan MAT-1020B instrument. Elemental analyses were carried out with a

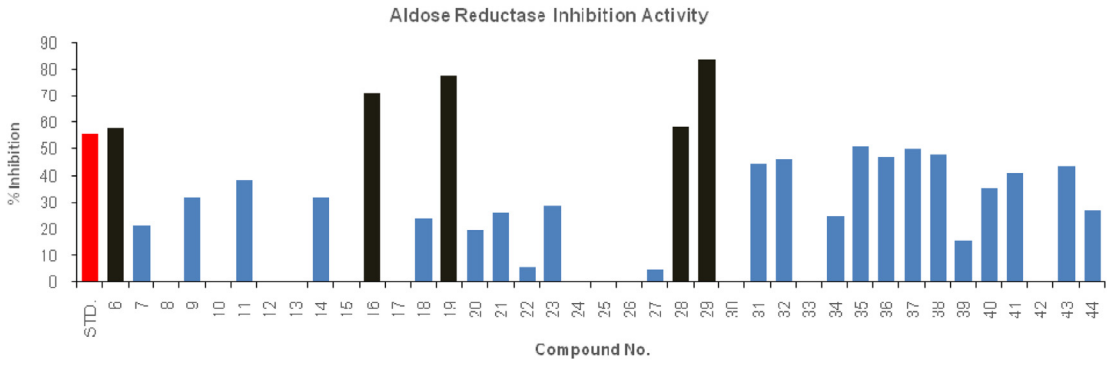

Fig. 6. Aldose reductase inhibitory activity of new epalrestat analogues (1 μM in DMSO). Standard Drug: epalrestat (1 μM in DMSO).

Table 4
Prediction of interactions of compounds in the active site of aldose reductase in FlexX.

S. no.	Compound	Protein–ligand interaction	Type of interactions
1	Co-crystal (Tolrestat)	Y48, H110, W111	Hydrogen bonding
2	Epalrestat[a]	Y48, H110, W111	Hydrogen bonding
3	6	Y48, H110, W111	Hydrogen bonding
4	16	Y48, H110, W111, S302	Hydrogen bonding
5	19	F122, L300, W79, W111, W20, W219	Hydrophobic & π–π interactions
6	28	A299, L300, W219, C298, S302	Hydrophobic & π–π interactions
7	29	Y48, H110, W111, S302	Hydrogen bonding

[a] Reference compound used for *in vitro* activity assay.

Perkin Elmer 2400 Series II elemental analyzer. Column chromatography was performed on silica gel (60–120 mesh, Acme, India).

4.2. General procedure for the synthesis of Baylis–Hillman adducts

Aromatic aldehydes (**2a**–**2l**) (10 mmol), acrylonitrile (**3**) (20 mmol) and DABCO (30 mol% with respect to aldehyde) were mixed and allowed to stir at room temperature until completion of the reaction (10–12 h). Upon completion, the reaction mixture was diluted with water (15 mL) and extracted with diethylether (3 × 25 mL). The combined organic layers were dried over Na_2SO_4, concentrated under reduced pressure and purified by column chromatography using 10% EtOAc in hexane as eluent to afford pure Baylis–Hillman adducts (**4a**–**4l**) in 80–90% yield. The spectroscopic and analytical data of all the synthesized compounds were in good agreement with those reported in the literature [22].

4.3. General procedure for the synthesis of [E]-α-cyanocinnamaldehyde (**5a**–**5l**) [23a]

A stirred solution of BH adduct (**4a**–**4l**) (3 mmol) and $NaNO_3$ (3 mmol) in 3 mL of [Hmim] HSO_4 was heated at 80 °C for 1–2 h. The reaction progress was monitored by TLC. Upon completion, the reaction mixture was cooled to RT and extracted with ethylacetate (3 × 15 mL). The combined organic layers were dried over Na_2SO_4, filtered and evaporated under reduced pressure. The resulting crude product was purified by column chromatography using 10% EtOAc in hexane as eluent to afford pure [*E*]-α-cyanocinnamaldehyde derivatives (**5a**–**5l**). The characterization data of the newly synthesized compounds were given below.

4.3.1. (E)-3-(4-Ethylphenyl)-2-formylacrylonitrile (**5c**)

White solid; Yield: 75%; mp: 53–56 °C; ^{1}H NMR (300 MHz, $CDCl_3$): δ 9.55 (s, 1H), 7.96 (d, *J* = 8.3 Hz, 2H), 7.83 (s, 1H), 7.37 (d, *J* = 8.3 Hz, 2H), 2.79–2.72 (q, *J* = 7.5 Hz, 2H), 1.30 (t, *J* = 7.5 Hz, 3H); ^{13}C NMR (75 MHz, $CDCl_3$): δ 187.0, 159.0, 152.1, 131.6, 129.1, 128.8, 114.3, 111.1, 29.1, 14.8; MS (ESI) *m*/*z* (%): 186 $[M + H]^+$.

4.3.2. (E)-3-(4-Fluorophenyl)-2-formylacrylonitrile (**5f**)

White solid; Yield: 77%; mp: 105–109 °C; ^{1}H NMR (300 MHz, $CDCl_3$): δ 9.60 (s, 1H), 8.26 (s, 1H), 8.16–8.11 (m, 2H), 7.26 (t, *J* = 8.4 Hz, 2H); ^{13}C NMR (75 MHz, $CDCl_3$): δ 185.7, 149.5, 148.5, 141.7, 123.5, 114.5; MS (ESI) *m*/*z* (%): 176 $[M + H]^+$.

4.3.3. (E)-3-(4-Bromophenyl)-2-formylacrylonitrile (**5h**)

White solid; Yield: 75%; mp: 133–137 °C; ^{1}H NMR (300 MHz, $CDCl_3$): δ 9.57 (s, 1H), 7.90 (d, *J* = 9.0 Hz, 2H), 7.81 (s, 1H), 7.70 (d, *J* = 9.0 Hz, 2H); ^{13}C NMR (75 MHz, $CDCl_3$): δ 186.3, 157.2, 132.9, 132.4, 129.9, 129.5, 113.9, 112.7; MS (ESI) *m*/*z* (%): 237 $[M + H]^+$.

4.3.4. (E)-2-Formyl-3-(furan-2-yl)acrylonitrile (**5k**)

Yellow solid; Yield: 68%; mp: 158–163 °C; ^{1}H NMR (300 MHz, $CDCl_3$): δ 9.51 (s, 1H), 7.82 (d, *J* = 1.5 Hz, 1H), 7.70 (s, 1H), 7.57 (d, *J* = 3.7 Hz, 1H), 6.74–6.72 (dd, *J* = 1.5 Hz, 3.7 Hz, 1H); ^{13}C NMR (75 MHz, $CDCl_3$): δ 185.7, 149.5, 148.5, 141.7, 123.5, 114.5, 107.7; MS (ESI) *m*/*z* (%): 148 $[M + H]^+$.

4.4. General procedure for the synthesis of epalrestat analogues (**6**–**44**)

A mixture of rhodanine (3 mmol), substituted [*E*]-α-cyanocinnamaldehyde (3 mmol) and anhydrous ammonium acetate (3 mmol) were taken in glacial acetic acid (10 mL). The reaction mixture was heated to 120 °C in an oil bath for 3–4 h. The reaction was monitored by TLC. Upon completion, the reaction mixture was cooled, filtered and washed with water. Finally it was recrystallized from methanol to yield pure compounds.

4.4.1. 2-((Z)-5-((Z)-2-Cyano-3-phenylallylidene)-4-oxo-2-thioxothiazolidin-3-yl)acetic acid (**6**)

Yellow solid; Yield: 81%; mp: 255–260 °C; ^{1}H NMR (300 MHz, DMSO-d_6): δ 8.31 (s, 1H), 7.93 (d, *J* = 7.1 Hz, 2H), 7.67 (s, 1H), 7.62–7.58 (m, 3H), 4.70 (s, 2H); ^{13}C NMR (75 MHz, DMSO-d6): δ 192.6, 167.1, 166.1, 156.0, 132.9, 132.7, 130.9, 129.9, 129.4, 123.6, 116.5, 104.9, 44.9; IR (KBr, cm^{-1}): 2968, 2217, 1717, 1581, 1440, 1326, 1252, 1193, 740; MS (ESI) *m*/*z* (%): 331 $[M + H]^+$; Anal. Calcd for $C_{15}H_{10}N_2O_3S_2$: C, 54.53; H, 3.05; N, 8.4; S, 19.41; Found: C, 54.56; H, 3.07; N, 8.46; S, 19.46.

4.4.2. 2-((Z)-5-((Z)-2-Cyano-3-p-tolylallylidene)-4-oxo-2-thioxothiazolidin-3-yl)acetic acid (**7**)

Thick yellow solid; Yield: 83%; mp: 273–280 °C; ^{1}H NMR (300 MHz, DMSO-d_6): δ 8.14 (s, 1H), 7.85 (d, *J* = 7.9 Hz, 2H), 7.65 (s, 1H), 7.35 (d, *J* = 7.7 Hz, 2H), 4.70 (s, 2H), 2.43 (s, 3H); ^{13}C NMR (75 MHz, DMSO-d_6): δ 192.6, 167.1, 166.1, 156.0, 143.9, 131.2, 130.1, 130.0, 122.9, 116.7, 103.6, 44.9, 21.3; IR (KBr, cm^{-1}): 3373, 2925,

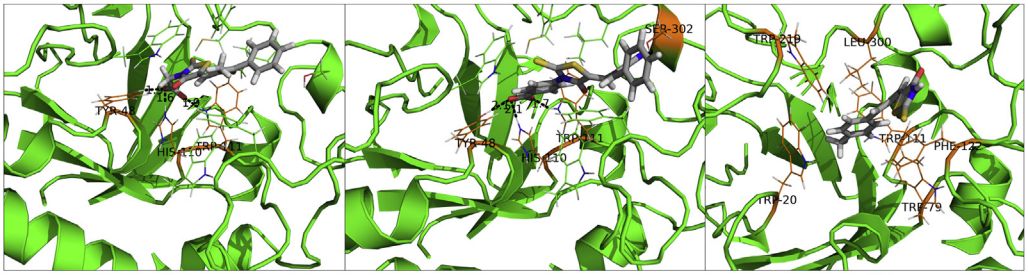

6 29 19

Fig. 8. Docking poses for some most active compounds (amino acids of receptor having interactions with docked ligands are coloured in orange; Hydrogen bonding of SER302 in compound **29** is not clearly visible).

2216, 1572, 1395, 1321, 1255, 1191, 742; MS (ESI) *m/z* (%): 345 $[M + H]^+$; Anal. Calcd for $C_{16}H_{12}N_2O_3S_2$: C, 55.80; H, 3.51; N, 8.13; S, 18.62; Found: C, 55.81; H, 3.55; N, 8.16; S, 18.60.

*4.4.3. 2-((Z)-5-((Z)-2-Cyano-3-(4-ethylphenyl)allylidene)-4-oxo-2-thioxothiazolidin-3-yl)acetic acid (**8**)*

Yellow solid; Yield: 80%; mp: 275–279 °C; ^{1}H NMR (300 MHz, DMSO-d_6): δ 8.00 (s, 1H), 7.88 (d, *J* = 7.9 Hz, 2H), 7.61 (s, 1H), 7.34 (d, *J* = 7.9 Hz, 2H), 7.71 (s, 2H), 4.71 (s, 2H), 2.76–2.69 (q, *J* = 7.5 Hz, 2H), 1.27 (t, *J* = 7.5 Hz, 3H); ^{13}C NMR (75 MHz, DMSO-d_6): δ 192.5, 167.0, 166.1, 156.0, 149.8, 131.2, 130.3, 130.2, 128.8, 122.9, 116.6, 103.7, 44.9, 28.2, 14.9; IR (KBr, cm^{-1}): 3411, 2966, 2928, 2215, 1720, 1572, 1395, 1327, 1250, 1196, 742; MS (EI) *m/z* (%): 358 $[M]^+$; Anal. Calcd for $C_{17}H_{14}N_2O_3S_2$: C, 56.96; H, 3.94; N, 7.82; S, 17.89; Found: C, 56.95; H, 3.95; N, 7.87; S, 17.87.

*4.4.4. 2-((Z)-5-((Z)-2-Cyano-3-(4-isopropylphenyl)allylidene)-4-oxo-2-thioxothiazolidin-3-yl)acetic acid (**9**)*

Thick yellow solid; Yield: 82%; mp: 266–272 °C; ^{1}H NMR (300 MHz, DMSO-d_6): δ 8.26 (s, 1H), 7.89 (d, *J* = 8.1 Hz, 2H), 7.66 (s, 1H), 7.48 (d, *J* = 8.1 Hz, 2H), 4.72 (s, 2H), 3.03–2.93 (m, *J* = 6.7 Hz, 1H), 1.23 (d, *J* = 6.7 Hz, 6H); ^{13}C NMR (75 MHz, DMSO-d_6): δ 193.5, 167.1, 165.7, 156.0, 154.3, 131.2, 130.5, 130.3, 127.4, 126.5, 122.9, 116.7, 44.9, 33.6, 23.3; IR (KBr, cm^{-1}): 3421, 2961, 2926, 2216, 1712, 1571, 1389, 1327, 1247, 1196, 742; MS (EI) *m/z* (%): 372 $[M]^+$; Anal. Calcd for $C_{18}H_{16}N_2O_3S_2$: C, 58.04; H, 4.33; N, 7.52; S, 17.22; Found: C, 58.08; H, 4.39; N, 7.56; S, 17.20.

*4.4.5. 2-((Z)-5-((Z)-2-Cyano-3-(4-methoxyphenyl)allylidene)-4-oxo-2-thioxothiazolidin-3-yl)acetic acid (**10**)*

Thick yellow solid; Yield: 68%; mp: 303–308 °C; ^{1}H NMR (300 MHz, DMSO-d_6): δ 8.20 (s, 1H), 7.94 (d, *J* = 8.5 Hz, 2H), 7.61 (s, 2H), 7.10 (d, *J* = 8.5 Hz, 2H), 4.65 (s, 2H), 3.86 (s, 3H); ^{13}C NMR (75 MHz, DMSO-d_6): δ 192.6, 167.1, 166.2, 163.2, 155.8, 132.6, 131.8, 125.4, 121.6, 117.1, 115.1, 101.3, 55.7, 45.0; IR (KBr, cm^{-1}): 2974, 2934, 2212, 1720, 1570, 1394, 1324, 1203, 1179, 741; MS (EI) *m/z* (%): 360 $[M]^+$; Anal. Calcd for $C_{16}H_{12}N_2O_4S_2$: C, 53.32; H, 3.36; N, 7.77; S, 17.79; Found: C, 53.27; H, 3.41; N, 7.81; S, 17.71.

*4.4.6. 2-((Z)-5-((Z)-2-Cyano-3-(4-fluorophenyl)allylidene)-4-oxo-2-thioxothiazolidin-3-yl)acetic acid (**11**)*

Yellow solid; Yield: 74%; mp: 240–245 °C; ^{1}H NMR (300 MHz, DMSO-d_6): δ 7.86 (s, 1H), 7.72–7.67 (m, *J* = 8.3 Hz, 5.4 Hz, 2H), 7.36–7.29 (m, *J* = 8.3 Hz, 5.4 Hz, 3H), 4.71 (s, 2H); ^{13}C NMR (75 MHz, DMSO-d_6): δ 193.0, 167.3, 166.3, 164.9, 161.5, 133.3, 133.2, 132.6, 129.4, 121.5, 116.8, 116.5, 45.2; IR (KBr, cm^{-1}): 3178, 3002, 2960, 1734, 1678, 1587, 1411, 1345, 1186, 1158, 744; MS (ESI) *m/z* (%): 371 $[M + Na]^+$; Anal. Calcd for $C_{15}H_9FN_2O_3S_2$: C, 51.71; H, 2.60; N, 8.04; S, 18.41; Found: C, 51.70; H, 2.62; N, 8.03; S, 18.45.

*4.4.7. 2-((Z)-5-((Z)-3-(4-Chlorophenyl)-2-cyanoallylidene)-4-oxo-2-thioxothiazolidin-3-yl)acetic acid (**12**)*

Green solid; Yield: 72%; mp: 250–256 °C; ^{1}H NMR (300 MHz, DMSO-d_6): δ 7.75 (s, 1H), 7.58–7.46 (m, 5H), 4.74 (s, 2H); ^{13}C NMR (75 MHz, DMSO-d_6): δ 192.8, 166.7, 166.2, 154.2, 135.8, 132.4, 132.2, 131.6, 131.5, 130.5, 129.5, 122.4, 44.9; IR (KBr, cm^{-1}): 3017, 2938, 1712, 1598, 1401, 1331, 1185, 1092, 743; MS (ESI) *m/z* (%): 365 $[M + H]^+$; Anal. Calcd for $C_{15}H_9ClN_2O_3S_2$: C, 49.38; H, 2.49; N, 7.68; S, 17.58; Found: C, 49.38; H, 2.49; N, 7.69; S, 17.59.

*4.4.8. 2-((Z)-5-((Z)-3-(4-Bromophenyl)-2-cyanoallylidene)-4-oxo-2-thioxothiazolidin-3-yl)acetic acid (**13**)*

Yellow solid; Yield: 73%; mp: 275–279 °C; ^{1}H NMR (300 MHz, DMSO-d_6): δ 8.22 (s, 1H), 7.85 (d, *J* = 7.9 Hz, 2H), 7.74 (d, *J* = 7.9 Hz, 2H), 7.64 (s, 1H), 4.71 (s, 2H); ^{13}C NMR (75 MHz, DMSO-d_6): δ 192.5, 167.1, 166.1, 154.4, 132.5, 131.8, 131.6, 130.5, 126.5, 124.1, 116.3, 105.6, 44.9; IR (KBr, cm^{-1}): 3415, 2923, 2652, 2211, 1717, 1567, 1362, 1331, 1193, 1116, 739; MS (ESI) *m/z* (%): 431 $[M + Na]^+$; Anal. Calcd for $C_{15}H_9BrN_2O_3S_2$: C, 44.02; H, 2.22; N, 6.84; S, 15.67; Found: C, 44.02; H, 2.24; N, 6.87; S, 15.68.

*4.4.9. 2-((Z)-5-((Z)-2-Cyano-3-(naphthalen-1-yl)allylidene)-4-oxo-2-thioxothiazolidin-3-yl)acetic acid (**14**)*

Thick yellow solid; Yield: 75%; mp: 279–283 °C; ^{1}H NMR (300 MHz, DMSO-d_6): δ 8.95 (s, 1H), 8.25 (d, *J* = 7.5 Hz, 2H), 8.05 (d, *J* = 7.5 Hz, 1H), 7.95–7.90 (m, 2H), 7.64–7.56 (m, 3H), 4.74 (s, 2H); ^{13}C NMR (75 MHz, DMSO-d_6): δ 192.6, 167.0, 166.1, 153.7, 133.0, 132.8, 131.0, 130.9, 129.7, 128.8, 127.7, 127.0, 126.8, 125.4, 123.8, 123.5, 116.4, 107.8, 44.9; IR (KBr, cm^{-1}): 3422, 2928, 2218, 1737, 1717, 1398, 1330, 1200, 1120, 738; MS (ESI) *m/z* (%): 381 $[M + H]^+$; Anal. Calcd for $C_{19}H_{12}N_2O_3S_2$: C, 59.98; H, 3.18; N, 7.36; S, 16.86; Found: C, 59.96; H, 3.18; N, 7.36; S, 16.89.

*4.4.10. 2-((Z)-5-((Z)-2-Cyano-3-(4-(trifluoromethyl)phenyl) allylidene)-4-oxo-2-thioxothiazolidin-3-yl)acetic acid (**15**)*

Yellow solid; Yield: 72%; mp: 242–245 °C; ^{1}H NMR (300 MHz, DMSO-d_6): δ 8.07 (d, *J* = 7.8 Hz, 2H), 8.04 (s, 1H), 7.77 (d, *J* = 7.8 Hz, 2H), 7.60 (s, 1H), 4.73 (s, 2H); ^{13}C NMR (75 MHz, DMSO-d_6): δ 192.5, 167.0, 166.1, 153.7, 136.4, 131.8, 131.1, 130.3, 129.9, 126.1, 125.3, 116.0, 107.8, 44.9; IR (KBr, cm^{-1}): 3024, 2932, 2217, 1716, 1584, 1399, 1325, 1200, 1125, 740; MS (ESI) *m/z* (%): 421 $[M + Na]^+$; Anal. Calcd for $C_{16}H_9F_3N_2O_3S_2$: C, 48.24; H, 2.28; N, 7.03; S, 16.10; Found: C, 48.31; H, 2.15; N, 7.08; S, 16.16.

*4.4.11. 2-((Z)-5-((Z)-2-Cyano-3-(furan-2-yl)allylidene)-4-oxo-2-thioxothiazolidin-3-yl)acetic acid (**16**)*

Dark red solid; Yield: 79%; mp: 256–260 °C; ^{1}H NMR (300 MHz, DMSO-d_6): δ 8.21 (s, 1H), 8.09 (brs, 1H), 7.65 (s, 1H), 7.40 (d, *J* = 3.6 Hz, 1H), 6.87 (m, 1H), 4.71 (s, 2H); ^{13}C NMR (75 MHz, DMSO-d_6): δ 192.4, 167.1, 166.1, 149.6, 149.3, 139.6, 130.9, 122.4, 116.3, 114.6, 114.1, 100.3, 44.9; IR (KBr, cm^{-1}): 3139, 3041, 2656, 2210, 1718, 1570, 1451, 1366, 1251, 1190, 742; MS (ESI) *m/z* (%): 343 $[M + Na]^+$; Anal. Calcd for $C_{13}H_8N_2O_4S_2$: C, 48.74; H, 2.52; N, 8.74; S, 20.02; Found: C, 48.75; H, 2.52; N, 8.75; S, 20.06.

*4.4.12. 2-((Z)-5-((Z)-2-Cyano-3-(thiophen-2-yl)allylidene)-4-oxo-2-thioxothiazolidin-3-yl)acetic acid (**17**)*

Orange solid; Yield: 80%; mp: 277–283 °C; ^{1}H NMR (300 MHz, DMSO-d_6): δ 8.37 (s, 1H), 8.01 (d, *J* = 4.7 Hz, 1H), 7.82 (d, *J* = 3.3 Hz, 1H), 7.62 (s, 1H), 7.27 (t, *J* = 4.7 Hz, 3.3 Hz, 1H), 4.70 (s, 2H); ^{13}C NMR (75 MHz, DMSO-d_6): δ 192.4, 167.1, 166.1, 148.2, 138.1, 137.0, 136.4, 130.7, 129.0, 122.2, 116.6, 101.0, 45.0; IR (KBr, cm^{-1}): 3407, 3022, 2963, 2221, 1710, 1589, 1407, 1369, 1208, 1180, 733; MS (EI) *m/z* (%): 336 $[M]^+$; Anal. Calcd for $C_{13}H_8N_2O_3S_3$: C, 46.41; H, 2.40; N, 8.33; S 28.59; Found: C, 46.46; H, 2.40; N, 8.25; S, 28.55.

*4.4.13. (Z)-2-((Z)-(4-Oxo-2-thioxothiazolidin-5-ylidene)methyl)-3-phenylacrylonitrile (**18**)*

Brown solid; Yield: 68%; mp: 250–255 °C; ^{1}H NMR (300 MHz, DMSO-d_6): δ 7.91 (s, 1H), 7.81–7.65 (m, 2H), 7.55–7.46 (m, 3H), 7.32 (s, 1H); ^{13}C NMR (75 MHz, DMSO-d_6): δ 195.2, 169.1, 154.8, 132.8, 132.5, 129.7, 129.2, 128.4, 127.7, 116.4, 105.1; IR (KBr, cm^{-1}): 3441, 3118, 2844, 2213, 1727, 1576, 1554, 1433, 1288, 1181, 742; MS (EI) *m/z* (%): 272 $[M]^+$; Anal. Calcd for $C_{13}H_8N_2OS_2$: C, 57.33; H, 2.96; N, 10.29; S, 23.55; Found: C, 57.30; H, 2.92; N, 10.30, S, 23.58.

*4.4.14. (Z)-2-((Z)-(4-Oxo-2-thioxothiazolidin-5-ylidene)methyl)-3-p-tolylacrylonitrile (**19**)*

Orange solid; Yield: 70%; mp: 264–267 °C; ^{1}H NMR (300 MHz, DMSO-d_6): δ 13.51 (s, 1H), 7.84–7.81 (m, 3H), 7.33 (s, 1H), 7.30 (d,

J = 7.0 Hz, 2H), 2.43 (s, 3H); ^{13}C NMR (75 MHz, DMSO-d_6): δ 195.1, 169.1, 154.8, 143.4, 139.2, 130.1, 129.9, 128.7, 126.9, 116.6, 103.8, 21.2; IR (KBr, cm^{-1}): 3447, 3148, 3051, 2998, 2210, 1686, 1567, 1422, 1302, 1177, 1064, 808; MS (ESI) m/z (%): 309 [M + Na]$^+$; Anal. Calcd for $C_{14}H_{10}N_2OS_2$: C, 58.72; H, 3.52; N, 9.78; S, 22.39; Found: C, 58.60; H, 3.50; N, 9.50; S, 22.51.

4.4.15. (Z)-3-(4-Ethylphenyl)-2-((Z)-(4-oxo-2-thioxothiazolidin-5-ylidene)methyl)acrylonitrile (**20**)

Orange solid; Yield: 73%; mp: 252–256 °C; ^{1}H NMR (300 MHz, DMSO-d_6): δ 13.48 (s, 1H), 7.85 (d, J = 8.0 Hz, 2H), 7.78 (s, 1H), 732–7.30 (m, 3H), 2.74–2.69 (q, J = 7.0 Hz, 2H), 1.27 (t, J = 7.00 Hz, 3H); ^{13}C NMR (75 MHz, DMSO-d_6): δ 195.1, 169.1, 154.9, 149.4, 130.4, 130.0, 128.8, 128.7, 126.9, 116.6, 103.8, 28.2, 14.9; IR (KBr, cm^{-1}): 3445, 3149, 2998, 2962, 2211, 1688, 1567, 1422, 1303, 1205, 1178, 1064, 822; MS (EI) m/z (%): 300 [M]$^+$; Anal. Calcd for $C_{15}H_{12}N_2OS_2$: C, 59.97; H, 4.03; N, 9.33; S, 21.35; Found: C, 59.97; H, 4.05; N, 9.34; S, 21.36.

4.4.16. (Z)-3-(4-Isopropylphenyl)-2-((Z)-(4-oxo-2-thioxothiazolidin-5-ylidene)methyl)acrylonitrile (**21**)

Brown solid; Yield: 73%; mp: 240–244 °C; ^{1}H NMR (300 MHz, DMSO-d_6): δ 13.58 (brs, 1H), 7.91 (s, 1H), 7.86 (d, J = 7.9 Hz, 2H), 7.36–7.34 (m, 3H), 3.00–2.93 (m, 1H), 1.28 (d, J = 6.7 Hz, 6H); ^{13}C NMR (75 MHz, DMSO-d_6): δ 195.2, 169.1, 154.9, 153.9, 130.6, 130.1, 128.8, 127.3, 126.9, 116.7, 103.9, 33.5, 23.3; IR (KBr, cm^{-1}): 3423, 3010, 2957, 2214, 1694, 1576, 1433, 1301, 1182, 1058, 823; MS (EI) m/z (%): 314 [M]$^+$; Anal. Calcd for $C_{16}H_{14}N_2OS$: C, 61.12; H, 4.49; N, 8.91; S, 20.40; Found: C, 61.11; H, 4.51; N, 8.93; S, 20.42.

4.4.17. (Z)-3-(4-Methoxyphenyl)-2-((Z)-(4-oxo-2-thioxothiazolidin-5-ylidene)methyl)acrylonitrile (**22**)

Orange solid; Yield: 69%; mp: 294–299 °C; ^{1}H NMR (300 MHz, DMSO-d_6): δ 13.60 (s, 1H), 7.95 (d, J = 7.9 Hz, 2H), 7.92 (s, 1H), 7.36 (s, 1H), 7.05 (d, J = 7.9 Hz, 2H), 3.88 (s, 3H); ^{13}C NMR (75 MHz, DMSO-d_6): δ 195.1, 169.1, 162.9, 154.6, 132.3, 129.4, 125.6, 125.5, 116.9, 114.9, 101.5, 55.6; IR (KBr, cm^{-1}): 3406, 3095, 2845, 2213, 1713, 1549, 1507, 1446, 1311, 1275, 1178, 1015, 744; MS (EI) m/z (%): 302 [M]$^+$; Anal. Calcd for $C_{14}H_{10}N_2O_2S_2$: C, 55.61; H, 3.33; N, 9.26; S, 21.21; Found: C, 55.68; H, 3.35; N, 9.30; S, 21.25.

4.4.18. (Z)-3-(4-Fluorophenyl)-2-((Z)-(4-oxo-2-thioxothiazolidin-5-ylidene)methyl)acrylonitrile (**23**)

Yellow solid; Yield: 68%; mp: 288–293 °C; ^{1}H NMR (300 MHz, DMSO-d_6): δ 13.52 (brs, 1H), 8.00–7.96 (m, 2H), 7.85 (s, 1H), 7.32 (s, 1H), 7.23–7.18 (t, 3H); ^{13}C NMR (75 MHz, DMSO-d_6): δ 195.2, 169.1, 163.3, 153.4, 135.0, 132.5, 132.4, 128.3, 116.7, 116.4, 104.8; IR (KBr, cm^{-1}): 3441, 3010, 2853, 2210, 1697, 1573, 1501, 1436, 1302, 1235, 1191, 829; MS (EI) m/z (%): 290 [M]$^+$; Anal. Calcd for $C_{13}H_7FN_2OS_2$: C, 53.78; H, 2.43; N, 9.65; S, 22.09; Found: C, 53.81; H, 2.48; N, 9.71; S, 22.11.

4.4.19. (Z)-3-(4-Chlorophenyl)-2-((Z)-(4-oxo-2-thioxothiazolidin-5-ylidene)methyl)acrylonitrile (**24**)

Yellow solid; Yield: 65%; mp: 265–269 °C; ^{1}H NMR (300 MHz, DMSO-d_6): δ 13.56 (brs, 1H), 7.90 (d, J = 8.6 Hz, 2H), 7.78 (s, 1H), 7.48 (d, J = 8.6 Hz, 2H), 7.34 (s, 1H); ^{13}C NMR (75 MHz, DMSO-d_6): δ 195.2, 167.4, 154.5, 136.0, 132.7, 132.5, 131.8, 129.8, 122.7, 116.2, 105.8; IR (KBr, cm^{-1}): 3422, 3226, 3016, 2215, 1716, 1569, 1434, 1300, 1227, 1186, 1093, 742; MS (EI) m/z (%): 306 [M]$^+$; Anal. Calcd for $C_{13}H_7ClN_2OS_2$: C, 50.89; H, 2.30; N, 9.13; S, 20.90; Found: C, 50.85; H, 2.32; N, 9.15; S, 20.90.

4.4.20. (Z)-3-(4-Bromophenyl)-2-((Z)-(4-oxo-2-thioxothiazolidin-5-ylidene)methyl)acrylonitrile (**25**)

Orange solid; Yield: 65%; mp: 244–248 °C; ^{1}H NMR (300 MHz, DMSO-d_6): δ 13.40 (brs, 1H), 7.79 (d, J = 8.0 Hz, 2H), 7.63 (d, J = 8.0 Hz, 2H), 7.57 (s, 1H), 7.25 (s, 1H); ^{13}C NMR (75 MHz, DMSO-d_6): δ 195.1, 169.1, 153.3, 132.4, 132.3, 131.9, 130.1, 128.1, 124.2, 116.2, 105.7; IR (KBr, cm^{-1}): 3568, 3096, 2857, 2220, 1721, 1563, 1447, 1304, 1231, 1184, 1067, 816; MS (EI) m/z (%): 351 [M]$^+$; Anal. Calcd for $C_{13}H_7BrN_2OS_2$: C, 44.45; H, 2.01; N, 7.98; S, 18.26; Found: C, 43.12; H, 1.95; N, 7.95; S, 17.48.

4.4.21. (Z)-3-(Aphthalene-1-yl)-2-((Z)-(4-oxo-2-thioxothiazolidin-5-ylidene)methyl)acrylonitrile (**26**)

Orange solid; Yield: 73%; mp: 255–260 °C; ^{1}H NMR (300 MHz, DMSO-d_6): δ 13.61 (s, 1H), 8.85 (s, 1H), 8.24–8.20 (t, J = 9.0 Hz, 7.0 Hz, 2H), 8.04 (d, J = 8.0 Hz, 1H), 7.94 (d, J = 8.0 Hz, 1H), 7.67 (s, 1H), 7.63–7.56 (m, 3H); ^{13}C NMR (75 MHz, DMSO-d_6): δ 195.2, 169.2, 152.7, 133.0, 132.5, 130.9, 129.8, 128.8, 128.5, 127.9, 127.6, 126.9, 126.8, 125.4, 123.5, 116.4, 108.1; IR (KBr, cm^{-1}): 3438, 3082, 2210, 1700, 1552, 1426, 1305, 1220, 1189, 1064, 787; MS (EI) m/z (%): 322 [M]$^+$; Anal. Calcd for $C_{17}H_{10}N_2OS_2$: C, 63.33; H, 3.13; N, 8.69; S, 19.89; Found: C, 62.34; H, 2.87; N, 8.03; S, 19.09.

4.4.22. (Z)-3-(Furan-2-yl)-2-((Z)-(4-oxo-2-thioxothiazolidin-5-ylidene)methyl)acrylonitrile (**27**)

Violet solid; Yield: 80%; mp: 284–289 °C; ^{1}H NMR (300 MHz, DMSO-d_6): δ 8.18 (d, J = 1.6 Hz, 1H), 8.00 (s, 1H), 7.40 (s, 1H), 7.35 (d, J = 3.6 Hz, 1H), 6.88–6.85 (dd, J = 3.6 Hz, 1.6 Hz, 1H); ^{13}C NMR (75 MHz, DMSO-d_6): δ 195.0, 169.0, 149.3, 149.1, 138.7, 128.4, 126.5, 121.5, 116.2, 114.3, 100.5; IR (KBr, cm^{-1}): 3451, 3127, 3033, 2848, 2215, 1684, 1564, 1440, 1355, 1391, 1204, 1150, 767; MS (EI) m/z (%): 262 [M]$^+$; Anal. Calcd for $C_{11}H_6N_2O_2S_2$: C, 50.37; H, 2.31; N, 10.68; S, 24.45; Found: C, 50.41; H, 2.29; N, 10.69; S, 24.44.

4.4.23. (Z)-2-((Z)-(4-Oxo-2-thioxothiazolidin-5-ylidene)methyl)-3-(thiophen-2-yl)acrylonitrile (**28**)

Thick solid; Yield: 81%; mp: 294–299 °C; ^{1}H NMR (300 MHz, DMSO-d_6): δ 8.42 (s, 1H), 8.15 (d, J = 5.2 Hz, 1H), 7.81 (d, J = 3.7 Hz, d), 7.37 (s, 1H), 7.35–7.32 (dd, J = 3.7 Hz, 5.2 Hz); ^{13}C NMR (75 MHz, DMSO-d_6): δ 195.0, 169.1, 147.1, 137.6, 137.0, 135.8, 128.9, 128.4, 126.3, 116.6, 101.2; IR (KBr, cm^{-1}): 3447, 3150, 3007, 2215, 1698, 1589, 1587, 1408, 1337, 1299, 1208, 1168, 723; MS (EI) m/z (%): 278 [M]$^+$; Anal. Calcd for $C_{11}H_6N_2OS_3$: C, 47.46; H, 2.17; N, 10.06; S, 34.56; Found: C, 47.50; H, 2.15; N, 10.08; S 34.60.

4.4.24. 4-((Z)-5-((Z)-2-Cyano-3-phenylallylidene)-4-oxo-2-thioxothiazolidin-3-yl)benzoic acid (**29**)

Yellow solid; Yield: 65%; mp: 265–270 °C; ^{1}H NMR (300 MHz, DMSO-d_6): δ 8.21 (d, J = 8.3 Hz, 2H), 7.81 (s, 1H), 7.61 (s, 1H), 7.59–7.50 (m, 5H), 7.41 (d, J = 8.3 Hz, 2H); ^{13}C NMR (75 MHz, DMSO-d_6): δ 193.6, 166.6, 166.4, 143.5, 138.8, 132.9, 132.7, 131.6, 130.9, 130.5, 130.4, 130.1, 129.4, 129.1, 123.2, 117.3; IR (KBr, cm^{-1}): 2921, 2672, 2210, 1722, 1691, 1599, 1427, 1340, 1244, 1154, 756; MS (EI) m/z (%): 392 [M]$^+$; Anal. Calcd for $C_{20}H_{12}N_2O_3S_2$: C, 61.21; H, 3.08; N, 7.14; S, 16.34; Found: C, 61.28; H, 3.10; N, 7.10; S, 16.39.

4.4.25. 4-((Z)-5-((Z)-2-Cyano-3-p-tolylallylidene)-4-oxo-2-thioxothiazolidin-3-yl)benzoic acid (**30**)

Yellow solid; Yield: 70%; mp: 284–286 °C; ^{1}H NMR (300 MHz, DMSO-d_6): δ 8.26 (s, 1H), 8.11 (d, J = 7.7 Hz, 2H), 7.85 (s, 1H), 7.62–7.53 (m, 4H), 7.41 (d, J = 7.3 Hz, 2H); ^{13}C NMR (75 MHz, DMSO-d_6): δ 193.6, 165.5, 155.5, 143.7, 141.4, 138.9, 138.6, 132.9, 131.6, 130.6, 130.4, 130.0, 129.1, 121.9, 117.3, 103.5, 21.1; IR (KBr, cm^{-1}): 2917, 2674, 2220, 1698, 1582, 1425, 1341,1293, 1241, 1156, 764; MS (EI) m/z (%): 406 [M]$^+$; Anal. Calcd for $C_{21}H_{14}N_2O_3S_2$: C, 62.05; H, 3.47; N, 6.89; S, 15.78; Found: C, 62.07; H, 3.42; N, 6.81; S, 15.71.

*4.4.26. 4-((Z)-5-((Z)-2-Cyano-3-(4-ethylphenyl)allylidene)-4-oxo-2-thioxothiazolidin-3-yl)benzoic acid (**31**)*

Yellow solid; Yield: 68%; mp: 288–293 °C; ^{1}H NMR (300 MHz, DMSO-d_6): δ 12.44 (s, 1H), 8.27 (s, 1H), 7.88 (d, J = 8.4 Hz, 2H), 7.61 (s, 1H), 7.45–7.42 (m, 4H), 7.34 (d, J = 8.4 Hz, 2H), 2.71–2.67 (q, J = 7.5 Hz, 2H), 1.21 (t, J = 7.5 Hz, 3H); ^{13}C NMR (75 MHz, DMSO-d_6): δ 193.0, 166.4, 155.5, 149.7, 147.4, 138.6, 132.8, 131.7, 130.7, 130.1, 129.0, 128.9, 128.8, 121.9, 116.7, 103.6, 28.0, 14.9; IR (KBr, cm^{-1}): 2960, 2250, 1692, 1580, 1422, 1347, 1288, 1245, 1158, 786; MS (EI) m/z (%): 420 [M]$^+$; Anal. Calcd for $C_{22}H_{16}N_2O_3S_2$: C, 62.84; H, 3.84; N, 6.66; S, 15.25; Found: C, 62.76; H, 3.79; N, 6.59; S, 15.21.

*4.4.27. 4-((Z)-5-((Z)-2-Cyano-3-(4-isopropylphenyl)allylidene)-4-oxo-2-thioxothiazolidin-3-yl)benzoic acid (**32**)*

Yellow solid; Yield: 69%; mp: 306–310 °C; ^{1}H NMR (300 MHz, DMSO-d_6): δ 12.43 (s, 1H), 8.27 (s, 1H), 7.88 (d, J = 7.5 Hz, 2H), 7.61 (s, 1H), 7.48 (d, J = 8.4 Hz, 2H), 7.44 (d, J = 7.5 Hz, 2H), 7.34 (d, J = 8.4 Hz, 2H), 3.02–2.93 (m, 1H), 1.24 (d, J = 6.6 Hz, 6H); ^{13}C NMR (75 MHz, DMSO-d_6): δ 193.5, 166.4, 155.4, 154.2, 151.9, 138.8, 132.8, 130.7, 130.0, 129.0, 127.5, 127.3, 124.6, 121.9, 116.7, 103.6, 33.3, 23.3; IR (KBr, cm^{-1}): 2957, 2664, 2216, 1698, 1589, 1545, 1422, 1349, 1247, 1158, 759; MS (EI) m/z (%): 434 [M]$^+$; Anal. Calcd for $C_{23}H_{18}N_2O_3S_2$: C, 63.57; H, 4.18; N, 6.45; S, 14.76; Found: C, 63.55; H, 4.25; N, 6.39; S, 14.79.

*4.4.28. 4-((Z)-5-((Z)-2-Cyano-3-(4-methoxyphenyl)allylidene)-4-oxo-2-thioxothiazolidin-3-yl)benzoic acid (**33**)*

Thick yellow solid; Yield: 65%; mp: 319–320 °C; ^{1}H NMR (300 MHz, DMSO-d_6): δ 8.18 (d, J = 7.7 Hz, 2H), 7.79–7.73 (m, 3H), 7.55 (s, 1H), 7.37 (d, J = 7.3 Hz, 2H), 7.03 (d, J = 7.7 Hz, 2H), 3.89 (s, 1H); ^{13}C NMR (75 MHz, DMSO-d_6): δ 193.0, 172.0, 166.4, 162.8, 154.9, 136.1, 133.1, 132.2, 130.0, 128.0, 125.2, 122.9, 116.8, 114.7, 101.0, 55.4; IR (KBr, cm^{-1}): 2969, 2675, 2212, 1715, 1693, 1579, 1552, 1312, 1268, 1236, 1181, 759; MS (EI) m/z (%): 422 [M]$^+$; Anal. Calcd for $C_{21}H_{14}N_2O_4S_2$: C, 59.70; H, 3.34; N, 6.63; S, 15.18; Found: C, 59.64; H, 3.38; N, 6.70; S, 15.17.

*4.4.29. 4-((Z)-5-((Z)-2-Cyano-3-(4-fluorophenyl)allylidene)-4-oxo-2-thioxothiazolidin-3-yl)benzoic acid (**34**)*

Yellow solid; Yield: 62%; mp: 293–299 °C; ^{1}H NMR (300 MHz, DMSO-d_6): δ 8.31 (s, 1H), 8.11 (d, J = 8.0 Hz, 2H), 8.02 (t, J = 9.0 Hz, 2H), 7.60 (s, 1H), 7.56 (d, J = 8.0 Hz, 2H), 7.47 (t, J = 9.0 Hz, 2H); ^{13}C NMR (75 MHz, DMSO-d_6): δ 193.0, 166.4, 165.1, 163.1, 154.0, 138.6, 133.1, 132.6, 131.7, 130.1, 129.4, 129.0, 125.3, 122.9, 116.7, 116.6, 104.5; IR (KBr, cm^{-1}): 3413, 3019, 2676, 2213, 1716, 1694, 1584, 1427, 1337, 1241, 1156, 762; MS (EI) m/z (%): 410 [M]$^+$; Anal. Calcd for $C_{20}H_{11}FN_2O_3S_2$: C, 58.53; H, 2.70; N, 6.83; S, 15.62; Found: C, 58.58; H, 2.72; N, 6.89; S, 15.63.

*4.4.30. 4-((Z)-5-((Z)-3-(4-Chlorophenyl)-2-cyanoallylidene)-4-oxo-2-thioxothiazolidin-3-yl)benzoic acid (**35**)*

Yellow solid; Yield: 65%; mp: 305–310 °C; ^{1}H NMR (300 MHz, DMSO-d_6): δ 8.20 (d, J = 7.7 Hz, 2H), 7.76 (s, 1H), 7.66 (s, 1H), 7.56–7.50 (m, 4H), 7.41 (d, J = 7.7 Hz, 2H); ^{13}C NMR (75 MHz, DMSO-d_6): δ 193.3, 166.4, 153.8, 140.0, 137.3, 135.5, 132.1, 131.7, 131.4, 131.2, 130.1, 129.5, 129.0, 123.99, 122.7, 109.4; IR (KBr, cm^{-1}): 2918, 2672, 2210, 1721, 1689, 1596, 1578, 1425, 1337, 1243, 1155, 765; MS (EI) m/z (%): 426 [M]$^+$; Anal. Calcd for $C_{20}H_{11}ClN_2O_3S_2$: C, 58.58; H, 2.72; N, 6.89; S, 15.63; Found: C, 57.70; H, 2.55; N, 6.58; S 15.05.

*4.4.31. 4-((Z)-5-((Z)-3-(4-Bromophenyl)-2-cyanoallylidene)-4-oxo-2-thioxothiazolidin-3-yl)benzoic acid (**36**)*

Yellow solid; Yield: 62%; mp: 300–305 °C; ^{1}H NMR (300 MHz, DMSO-d_6): δ 8.16 (d, J = 7.5 Hz, 2H), 8.04 (s, 1H), 7.86 (d, J = 7.7 Hz, 2H), 7.75 (s, 1H), 7.67 (d, J = 7.5 Hz, 1H), 7.40 (d, J = 7.7 Hz, 2H); ^{13}C NMR (75 MHz, DMSO-d_6): δ 193.4, 166.5, 153.9, 138.8, 135.3, 134.8, 132.5, 132.2, 131.5, 131.3, 130.1, 129.1, 126.8, 124.1, 118.7, 109.7; IR (KBr, cm^{-1}): 3008, 2671, 2210, 1719, 1691, 1570, 1425, 1336, 1241, 1155, 763; MS (EI) m/z (%): 471 [M]$^+$; Anal. Calcd for $C_{20}H_{11}BrN_2O_3S_2$: C, 50.96; H, 2.35; N, 5.94; S, 13.61; Found: C, 50.98; H, 2.32; N, 5.99; S, 13.58.

*4.4.32. 4-((Z)-5-((Z)-2-Cyano-3-(naphthalen-1-yl)allylidene)-4-oxo-2-thioxothiazolidin-3-yl)benzoic acid (**37**)*

Orange solid; Yield: 72%; mp: 270–274 °C; ^{1}H NMR (300 MHz, DMSO-d_6): δ 13.24 (brs, 1H), 8.34–8.27 (m, 2H), 8.23–8.06 (m, 5H), 7.95 (s, 1H), 7.77–7.66 (m, 3H), 7.63–7.58 (m, 2H); ^{13}C NMR (75 MHz, DMSO-d_6): δ 193.1, 166.5, 166.1, 153.2, 138.6, 133.1, 132.8, 131.7, 131.0130.1, 129.6, 129.1, 129.0, 128.8, 127.7, 127.0, 126.8, 125.7, 125.4, 123.5, 116.6, 107.7; IR (KBr, cm^{-1}): 3013, 2210, 1698, 1593, 1421, 1342, 1288, 1236, 1153, 773; MS (EI) m/z (%): 442 [M]$^+$; Anal. Calcd for $C_{24}H_{14}N_2O_3S_2$: C, 65.14; H, 3.19; N, 6.33; S, 14.49; Found: C, 65.21; H, 3.22; N, 6.38; S, 14.47.

*4.4.33. 4-((Z)-5-((Z)-2-Cyano-3-(furan-2-yl)allylidene)-4-oxo-2-thioxothiazolidin-3-yl)benzoic acid (**38**)*

Orange solid; Yield: 79%; mp: 298–302 °C; ^{1}H NMR (300 MHz, DMSO-d_6): δ 8.17 (d, J = 8.3 Hz, 2H), 7.87 (s, 1H), 7.73 (d, J = 5.0 Hz, 1H), 7.54 (s, 1H), 7.37–7.34 (m, 3H), 6.72–6.70 (m, 1H); ^{13}C NMR (75 MHz, DMSO-d_6): δ 192.9, 166.4, 163.2, 149.4, 149.3, 139.1, 138.7, 131.7, 130.1, 129.5, 129.0, 124.1, 122.0, 116.3, 114.5, 100.3; IR (KBr, cm^{-1}): 3031, 2676, 2217, 1695, 1571, 1452, 1427, 1335, 1293, 1229, 1153, 755; MS (EI) m/z (%): 382 [M]$^+$; Anal. Calcd for $C_{18}H_{10}N_2O_4S_2$: C, 56.53; H, 2.64; N, 7.33; S, 16.77; Found: C, 56.56; H, 2.65; N, 7.38; S, 16.81.

*4.4.34. 4-((Z)-5-((Z)-2-Cyano-3-(thiophen-2-yl)allylidene)-4-oxo-2-thioxothiazolidin-3-yl) benzoic acid (**39**)*

Orange solid; Yield: 79%; mp: 309–312 °C; ^{1}H NMR (300 MHz, DMSO-d_6): δ 13.18 (brs, 1H), 8.52 (s, 1H), 8.19 (d, J = 5.2 Hz, 1H), 8.10 (d, J = 8.3 Hz, 2H), 7.85 (d, J = 3.1 Hz, 1H), 7.60 (s, 1H), 7.56 (d, J = 8.3 Hz, 2H), 7.35 (t, J = 5.2 Hz, 3.1 Hz, 1H); ^{13}C NMR (75 MHz, DMSO-d_6): δ 192.9, 166.4, 163.9, 147.7, 138.7, 137.9, 137.0, 136.2, 131.7, 130.1, 129.5, 129.0, 129.0, 123.8, 116.7, 101.0; IR (KBr, cm^{-1}): 3441, 3017, 2675, 2213, 1695, 1563, 1411, 1337, 1295, 1239, 1152, 757; MS (EI) m/z (%): 398 [M]$^+$; Anal. Calcd for $C_{18}H_{10}N_2O_3S_3$: C, 54.25; H, 2.53; N, 7.03; S, 24.14; Found: C, 54.29; H, 2.55; N, 7.10; S, 24.09.

*4.4.35. 2-(4-((Z)-5-((Z)-2-Cyano-3-phenylallylidene)-4-oxo-2-thioxothiazolidin-3-yl)phenyl)acetic acid (**40**)*

Yellow solid; Yield: 72%; mp: 253–256 °C; ^{1}H NMR (300 MHz, DMSO-d_6): δ 7.96 (s, 1H), 7.81 (d, J = 8.0 Hz, 1H), 7.64 (s, 1H), 7.56–7.48 (m, 6H), 7.26–7.24 (m, 2H), 3.66 (s, 2H); ^{13}C NMR (75 MHz, DMSO-d_6): δ 193.8, 172.2, 166.6, 155.2, 136.3, 132.7, 132.5, 130.4, 130.2, 129.8, 129.4, 128.3, 125.3, 123.1, 116.5, 104.9, 40.1; IR (KBr, cm^{-1}): 3424, 3012, 2927, 2218, 1723, 1699, 1516, 1404, 1358, 1230, 1199, 1152, 754; MS (ESI) m/z (%): 407 [M + H]$^+$; Anal. Calcd for $C_{21}H_{14}N_2O_3S_2$: C, 62.05; H, 3.47; N, 6.89; S, 15.78; Found: C, 62.50; H, 3.50; N, 6.85; S, 15.65.

*4.4.36. 2-(4-((Z)-5-((Z)-2-Cyano-3-p-tolylallylidene)-4-oxo-2-thioxothiazolidin-3-yl)phenyl)acetic acid (**41**)*

Yellow solid; Yield: 75%; mp: 250–255 °C; ^{1}H NMR (300 MHz, DMSO-d_6): δ 8.03 (s, 1H), 7.88 (d, J = 8.1 Hz, 2H), 7.59 (s, 1H), 7.46 (d, J = 8.1 Hz, 2H), 7.35 (d, J = 8.1 Hz, 2H), 7.27 (d, J = 8.1 Hz, 2H), 3.66 (s, 2H), 2.43 (s, 3H); ^{13}C NMR (75 MHz, DMSO-d_6): δ 193.3, 172.3, 166.7, 155.4, 143.7, 136.4, 133.3, 132.7, 130.6, 130.3, 130.0, 129.8, 128.3, 124.5, 116.8, 103.6, 40.1, 21.3; IR (KBr, cm^{-1}): 3424, 3009, 2924, 2219, 1720, 1700, 1573, 1404, 1358, 1229, 1191, 1155, 809; MS (ESI) $m/$

z (%): 421 $[M + H]^+$; Anal. Calcd for $C_{22}H_{16}N_2O_3S_2$: C, 62.84; H, 3.84; N, 6.66; S, 15.25; Found: C, 61.87; H, 3.66; N, 6.09; S, 15.52.

4.4.37. 2-(4-((Z)-5-((Z)-2-Cyano-3-(4-ethylphenyl)allylidene)-4-oxo-2-thioxothiazolidin-3-yl) phenyl)acetic acid (**42**)

Yellow solid; Yield: 78%; mp: 266–271 °C; ^{1}H NMR (300 MHz, DMSO-d_6): δ 7.91 (d, J = 7.1 Hz, 2H), 7.85 (s, 1H), 7.54 (s, 1H), 7.49 (d, J = 7.1 Hz, 2H), 7.36 (d, J = 8.2 Hz, 2H), 7.25 (d, J = 8.2 Hz, 2H), 3.66 (s, 2H), 2.76–2.72 (q, J = 7.1 Hz, 2H), 1.28 (t, J = 7.1 Hz, 3H); ^{13}C NMR (75 MHz, DMSO-d_6): δ 193.3, 172.3, 166.7, 155.4, 149.7, 136.4, 133.3, 130.7, 130.3, 130.1, 129.8, 128.8, 128.3, 124.6, 116.8, 103.7, 40.1, 28.2, 14.9; IR (KBr, cm^{-1}): 3428, 2963, 2926, 2225, 1720, 1700, 1574, 1417, 1384, 1224, 1154, 814; MS (ESI) *m*/*z* (%): 435 $[M + H]^+$; Anal. Calcd for $C_{23}H_{18}N_2O_3S_2$: C, 63.57; H, 4.18; N, 6.45; S, 14.76; Found: C, 62.38; H, 3.96; N, 6.06; S, 14.95.

4.4.38. 2-(4-((Z)-5-((Z)-2-Cyano-3-(4-isopropylphenyl)allylidene)-4-oxo-2-thioxothiazolidin-3-yl)phenyl)acetic acid (**43**)

Yellow solid; Yield: 79%; mp: 265–269 °C; ^{1}H NMR (300 MHz, DMSO-d_6): δ 7.87 (d, J = 8.0 Hz, 2H), 7.81 (s, 1H), 7.49 (s, 1H), 7.44 (d, J = 7.1 Hz, 2H), 7.35 (d, J = 7.1 Hz, 2H), 7.20 (d, J = 8.0 Hz, 2H), 3.62 (s, 2H), 2.99–2.92 (m, 1H), 1.25 (d, J = 6.2 Hz, 6H); ^{13}C NMR (75 MHz, DMSO-d_6): δ 193.3, 172.3, 166.7155.4, 154.2, 136.4, 133.3, 130.5, 130.3, 130.2, 129.8, 128.3, 127.4, 124.6, 116.8, 103.7, 40.1, 33.6, 23.3; IR (KBr, cm^{-1}): 3426, 2958, 2950, 2223, 1720, 1702, 1577, 1515, 1358, 1224, 1154, 814; MS (ESI) *m*/*z* (%): 449 $[M + H]^+$; Anal. Calcd for $C_{24}H_{20}N_2O_3S_2$: C, 64.26; H, 4.49; N, 6.25; S, 14.30; Found: C, 64.80; H, 4.21; N, 6.30; S, 14.03.

4.4.39. 2-(4-((Z)-5-((Z)-2-cyano-3-(4-methoxyphenyl)allylidene)-4-oxo-2-thioxothiazolidin-3-yl)phenyl)acetic acid (**44**)

Orange solid; Yield: 75%; mp: 265–269 °C; ^{1}H NMR (300 MHz, DMSO-d_6): δ 7.99 (d, J = 8.3 Hz, 2H), 7.84 (s, 1H), 7.54 (s, 1H), 7.47 (d, J = 8.4 Hz, 2H), 7.25 (d, J = 8.3 Hz, 2H), 7.05 (d, J = 8.4 Hz, 2H), 3.91 (s, 3H), 3.66 (s, 2H); ^{13}C NMR (75 MHz, DMSO-d_6): δ 193.3, 172.3, 166.7, 163.1, 155.2, 136.4, 133.4, 132.5, 130.5, 130.3, 128.3, 125.5, 123.2, 117.1, 115.0, 101.3, 55.7, 40.1; IR (KBr, cm^{-1}): 3427, 2927, 2218, 1720, 1573, 1512, 1384, 1353, 1244, 1185, 734; MS (ESI) *m*/*z* (%): 437 $[M + H]^+$; Anal. Calcd for $C_{22}H_{16}N_2O_4S_2$: C, 60.53; H, 3.69; N, 6.42; S, 14.69; Found: C, 60.81; H, 3.07; N, 6.77; S, 14.34.

4.5. Aldose reductase inhibition assay protocol

Rat kidney tissue was utilized as a source of aldose reductase enzyme. Rat kidney tissue was homogenized in ice cold potassium phosphate buffer (50 mM, pH 7.4). The homogenate was centrifuged at 12,000 rpm at 40 °C for 30 min. The resulting supernatant was stored at −80 °C and used as a source of aldose reductase enzyme for further assay. The *in-vitro* assay of aldose reductase enzyme inhibition was performed according to the method described by Hayman and Kinoshita [31]. Assay mixture containing 0.1 M potassium phosphate buffer pH 6.2, 0.9 M DL-Glyceraldehyde (Sigma–Aldrich, USA), 2 M lithium sulphate (Acros Organics), mercapto ethanol (Biomatik), distilled water and 2 mM NADPH (Sigma–Aldrich, USA) was prepared. Test compound is incubated along with the enzyme for 20 min at 37 °C. Reaction mixture devoid of NADPH was added followed by incubation for 5 min at 37 °C, and used as a respective blank whose absorption has been recorded. The reaction was then initiated by addition of NADPH. The change in the absorbance at 340 nm due to NADPH oxidation was measured with the help of Lambda 25 UV–Visible Spectrophotometer. The inhibitory activity of test compounds was evaluated based on the decrease in the absorbance of NADPH at 340 nm and quantified using formula Inhibition% = 100-[T/C] × 100, where T = absorbance of test reaction and C = absorbance of control reaction. The therapeutic drug epalrestat was used as reference aldose reductase inhibitor. The inhibitory concentration 50% (IC_{50}) was calculated by nonlinear regression. The dose–response curve was obtained by plotting the percentage inhibition versus the concentrations.

4.6. Crystallographic data

X-ray data for the compound were collected at room temperature using a Bruker Smart Apex CCD diffractometer with graphite monochromated MoKα radiation (λ = 0.71073 Å) with ω-scan method [32]. Preliminary lattice parameters and orientation matrices were obtained from four sets of frames. Unit cell dimensions were determined using 5838 reflections for 39 data. Integration and scaling of intensity data was accomplished using SAINT program [32]. The structures were solved by Direct Methods using SHELXS97 [33] and refinement was carried out by full-matrix least-squares technique using SHELXL97 [33]. Anisotropic displacement parameters were included for all non-hydrogen atoms. All H atoms were positioned geometrically and treated as riding on their parent C atoms, with C–H distances of 0.93–0.97 Å, and with $U_{iso}(H) = 1.2U_{eq}$ (C) or $1.5U_{eq}$ for methyl atoms.

Crystal data for 39: $C_{18}H_{10}N_2O_4S_3 \cdot C_2H_6O_1S_1$ (1:1), M = 476.59, size 0.20 × 0.16 × 0.11 mm^3, triclinic, space group P-1 (No. 2), a = 8.6855(5), b = 9.9583(6), c = 12.7372(7) Å, α = 100.7990(10), β = 90.5890(10), γ = 100.0060(10)°, V = 1064.66(11) Å^3, Z = 2, D_c = 1.487 g/cm^3, F_{000} = 492, CCD area detector, Mo-Kα radiation, λ = 0.71073 Å, T = 293(2)K, $2\theta_{max}$ = 50.0°, 10355 reflections collected, 3747 unique (R_{int} = 0.0190). Final *GooF* = 1.059, R_1 = 0.0314, wR_2 = 0.0824, R indices based on 3378 reflections with I > 2 σ (I) (refinement on F^2), 277 parameters, μ = 0.477 mm^{-1}. CCDC 938773 contains the supplementary crystallographic data for this paper. These data can be obtained free of charge at www.ccdc.cam.ac.uk/conts/retrieving.html [or from the Cambridge Crystallographic Data Centre (CCDC), 12 Union Road, Cambridge CB2 1EZ, UK; fax: +44 (0) 1223 336 033; email: deposit@ccdc.cam.ac.uk].

Acknowledgements

The authors thank the Director, CSIR – Indian Institute of Chemical Technology (CSIR-IICT) for encouragement. VJR thanks CSC-0108-ORIGIN project. T.N.R. thanks UGC, M.R. thanks CSIR, New Delhi, for fellowships. SKB is thankful to Department of Biotechnology (DBT) for providing Ramalingaswami Fellowship, and CSIR for providing fund (SMiLE) and Senior Research Fellowship to PKB. KS and CB are thankful to Department of Pharmaceuticals, Govt of India for support and research fellowship respectively.

References

[1] (a) R.A. DeFronzo, Diabetologia 35 (1992) 389–397;
(b) R.D.G. Leslie, Eye 7 (1993) 205–208.
[2] (a) M.M. Engelgau, L.S. Geiss, J.B. Saaddine, J.P. Boyle, S.M. Benjamin, E.W. Gregg, E.F. Tierney, N. Rios-Burrows, A.H. Mokdad, E.S. Ford, G. Imperatore, K.M. Venkat Narayan, Ann. Intern. Med. 140 (2004) 945–950;
(b) K.M. Venkat Narayan, Clin. Diabetes 23 (2005) 51–52.
[3] S. Wild, G. Roglic, A. Green, R. Sicree, H. King, Diabetes Care 27 (2004) 1047–1053.
[4] (a) P.F. Kador, Med. Res. Rev. 8 (1988) 325–352;
(b) K.H. Gabbay, N. Engl. J. Med. 288 (1973) 831–836.
[5] (a) R.L. Engerman, Diabetes 38 (1989) 1203–1206;
(b) G.B. Reddy, A. Satyanarayana, N. Balakrishna, R. Ayyagari, M. Padma, K. Viswanath, J.M. Petrash, Mol. Vis. 14 (2008) 593–601.
[6] (a) R.J. Young, D.J. Ewing, B.F. Clarke, Diabetes 32 (1983) 938–942;
(b) P.J. Oates, Int. Rev. Neurobiol. 50 (2002) 325–392.
[7] (a) W.G. Robinson Jr., P.F. Kador, J.H. Kinoshita, Science 221 (1983) 1177–1179;
(b) R.V. Heyningen, Nature 184 (1959) 194–195.

[8] (a) M. Dunlop, Kidney Int. 58 (2000) S3–S12;
(b) A. Beyer-Mears, E. Cruz, T. Edelist, E. Varagiannis, Pharmacology 32 (1986) 52–60.
[9] (a) M. Pyörälä, H. Miettinen, P. Halonen, M. Laakso, K. Pyörälä, Arterioscler. Thromb. Vasc. Biol. 20 (2000) 538–544;
(b) J.A. Beckman, M.A. Creager, P. Libby, J. Am. Med. Assoc. 287 (2002) 2570–2581.
[10] (a) K.J. Wells-Knecht, D.V. Zyzak, J.E. Litchfield, S.R. Thorpe, J.W. Baynes, Biochemistry 34 (1995) 3702–3709;
b) H. Vlassara, M.R. Palace, J. Intern. Med. 251 (2002) 87–101;
(c) H. Kaneto, G. Xu, K.H. Song, K. Suzuma, S. Bonner-Weir, A. Sharma, G.C. Weir, J. Biol. Chem. 276 (2001) 31099–31104;
(d) T. Nishikawa, D. Edelstein, X.L. Du, S. Yamagishi, T. Matsumura, Y. Kaneda, M.A. Yorek, D. Beebe, P.J. Oates, H.P. Hammes, I. Giardino, M. Brownlee, Nature 404 (2000) 787–790.
[11] A.Y.W. Lee, S.S.M. Chung, FASEB J. 13 (1999) 23–30.
[12] (a) J.M. Jez, M.J. Bennett, B.P. Schlegel, M. Lewis, T.M. Penning, Biochem. J. 326 (1997) 625–636;
(b) J.H. Kinoshita, C. Nishimura, Diabetes Metab. Rev. 4 (1998) 323–337.
[13] M.A. Ramirez, N.L. Borja, Pharmacotherapy 28 (2008) 646–655.
[14] (a) A.M. Vincent, J.W. Russell, P. Low, E.L. Feldman, Endocr. Rev. 25 (2004) 612–628;
(b) S.K. Srivastava, K.V. Ramana, A. Bhatnagar, Endocr. Rev. 26 (2005) 380–392.
[15] (a) A.A. Tahrani, M.K. Piya, A. Kennedy, A.H. Barnett, Pharmacol. Ther. 125 (2010) 328–361;
(b) A.B. Olokoba, O.A. Obateru, L.B. Olokoba, Oman Med. J. 27 (2012) 269–273;
(c) L.P. Krall, V.A. Chabot, Med. Clin. North Am. 62 (1978) 681–694;
d) A.A. Tahrani, C.J. Bailey, S. Del Prato, A.H. Barnett, Lancet 378 (2011) 182–197.
[16] (a) P. Alexiou, K. Pegklidou, M. Chatzopoulou, I. Nicolaou, V.J. Demopoulos, Curr. Med. Chem. 16 (2009) 734–752;
(b) S. Suzen, E. Buyukbingol, Curr. Med. Chem. 10 (2003) 1329–1352.
[17] For recent publications on ARIs see: (a) A. Ramunno, S. Cosconati, S. Sartini, V. Maglio, S. Angiuoli, V.L. Pietra, S.D. Maro, M. Giustiniano, C.L. Motta, F.D. Settimo, L. Marinelli, E. Novellino, Eur. J. Med. Chem. 51 (2012) 216–226;
(b) R. Ottanà, R. Maccari, M. Giglio, A.D. Corso, M. Cappiello, U. Mura, S. Cosconati, L. Marinelli, E. Novellino, S. Sartini, C.L. Motta, F.D. Settimo, Eur. J. Med. Chem. 46 (2011) 2797–2806;
(c) M. Chatzopoulou, E. Mamadou, M. Juskova, C. Koukoulitsa, I. Nicolaou, M. Stefek, V.J. Demopoulos, Bioorg. Med. Chem. 19 (2011) 1426–1433;
(d) S. Ali, A. Saeed, N. Abbas, M. Shahid, M. Bolte, J. Iqbal, Med. Chem. Commun. 3 (2012) 1428–1434;
(e) T. Tomasic, L.P. Masic, Curr. Med. Chem. 16 (2009) 1596–1629;
(f) X. Chen, C. Zhu, F. Guo, X. Qiu, Y. Yang, S. Zhang, M. He, S. Parveen, C. Jing, Y. Li, B. Ma, J. Med. Chem. 53 (2010) 8330–8344;
(g) S. Zhang, X. Chen, S. Parveen, S. Hussain, Y. Yang, C. Jing, C. Zhu, ChemMedChem 8 (2013) 603–613;
(h) M. Eisenmann, H. Steuber, M. Zentgraf, M. Altenkamper, R. Ortmann, J. Perruchon, G. Klebe, M. Schlitzer, ChemMedChem 4 (2009) 809–819;
(i) Y. Yang, S. Zhang, B. Wu, M. Ma, X. Chen, X. Qin, M. He, S. Hussain, C. Jing, B. Ma, C. Zhu, ChemMedChem 7 (2012) 823–835;
(j) M. Scholz, M. Steinhagen, J.T. Heiker, A.G. Beck-Sickinger, E. Hey-Hawkins, ChemMedChem 6 (2011) 89–93;
(k) X. Chen, Y. Yang, B. Ma, S. Zhang, M. He, D. Gui, S. Hussain, C. Jing, C. Zhu, Q. Yu, Y. Liu, Eur. J. Med. Chem. 46 (2011) 1536–1544;
(l) D. Minehira, D. Takeda, H. Urata, A. Kato, I. Adachi, X. Wang, Y. Matsuya, K. Sugimoto, M. Takemura, S. Endo, T. Matsunaga, A. Hara, J. Koseki, K. Narukawa, S. Hirono, N. Toyooka, Bioorg. Med. Chem. 20 (2012) 356–367;
(m) R. Maccari, A.D. Corso, M. Giglio, R. Moschini, U. Mura, R. Ottanà, Bioorg. Med. Chem. Lett. 21 (2011) 200–203;
(n) V.R. Rao, P. Muthenna, G. Shankaraiah, C. Akileshwari, K.H. Babu, G. Suresh, K.S. Babu, R.S.C. Kumar, K.R. Prasad, P.A. Yadav, J.M. Petrash, G.B. Reddy, J.M. Rao, Eur. J. Med. Chem. 57 (2012) 344–361;
(o) N. Hotta, Y. Akanuma, R. Kawamori, K. Matsuoka, Y. Oka, M. Shichiri, T. Toyota, M. Nakashima, I. Yoshimura, N. Sakamoto, Y. Shigeta, Diabetes Care 29 (2006) 1538–1544;
(p) T.T. Takatsuki, M.K. Ibaraki, A.A. Osaka, T.M. Takatsuki, M.H. Takatsuki, H.T. Takatsuki, F.H. Suita, T.M. Otsu, U.S. Patent 4,464,382, 1984.
[18] (a) M.A. Pfeifer, M.P. Schumer, D.A. Gelber, Diabetes 46 (1997) S82–S89;
(b) N. Giannoukakis, Expert Opin. Invest. Drugs 17 (2008) 575–581.
[19] (a) P.F. Kador, J.H. Kinoshita, N.E. Sharpless, J. Med. Chem. 28 (1985) 841–849;
(b) R. Kikkawa, I. Hatanaka, H. Yasuda, N. Kobayashi, Y. Shigeta, H. Terashima, T. Morimura, M. Tsuboshima, Diabetologia 24 (1983) 290–292.
[20] (a) M. Ravinder, P.S. Sadhu, V.J. Rao, Tetrahedron Lett. 50 (2009) 4229–4232;
(b) M. Ravinder, P.S. Sadhu, A. Santhoshi, P. Narender, G.Y.S.K. Swamy, D. Ravikumar, V.J. Rao, Synthesis (2010) 573–578;
(c) P. Narender, B. Gangadasu, M. Ravinder, U. srinivas, G.Y.S.K. Swamy, K. Ravikumar, V.J. Rao, Tetrahedron 62 (2006) 954–959.
[21] (a) M. Ravinder, B. Mahendar, M. Saidulu, K.V. Hamsini, T.N. Reddy, Ch. Rohit, B. Sanjay Kumar, K. Srinivas, V.J. Rao, Bioorg. Med. Chem. Lett. 22 (2012) 6010–6015;
(b) P. Narender, U. Srinivas, M. Ravinder, Ch. Ramesh, B.A. Rao, K. Harakishore, B. Gangadasu, U.S.N. Murthy, V.J. Rao, Bioorg. Med. Chem. 14 (2006) 4600–4609;
(c) K. Srinivas, U. Srinivas, K. Bhanuprakash, K. Harakishore, U.S.N. Murthy, V.J. Rao, Eur. J. Med. Chem. 41 (2006) 1240–1246;
(d) B.A. Rao, R.S. Rajpoot, V.G.M. Naidu, K. Srinivas, S. Ramakrishna, V.J. Rao, Int. J. Pharm. Biol. Sci. 2 (2011) 191–202.
[22] (a) D. Basavaiah, B.S. Reddy, S.S. Badsara, Chem. Rev. 110 (2010) 5447–5674;
(b) V. Sing, S. Batra, Tetrahedron 64 (2008) 4511–4574.
[23] (a) L.D.S. Yadav, V.P. Srivastava, R. Patel, Tetrahedron Lett. 49 (2008) 3142–3146;
(b) D. Basavaiah, N. Kumaragurubaran, K. Padmaja, Synlett (1999) 1630–1632.
[24] (a) M. Azizmohammadi, M. Khoobi, A. Ramazani, S. Emami, A. Zarrin, O. Firuzi, R. Miri, A. Shafiee, Eur. J. Med. Chem. 59 (2013) 15–22;
(b) F.W.A. Barros, T.G. Silva, M.G. da Rocha Pitta, D.P. Bezerra, L.V. Costa-Lotufo, M.O. de Moraes, C. Pessoa, M.A. de Moura, F.C. de Abreu, C. de Lima Mdo, S.L. Galdino, I.D. Rocha Pitta, M.O. Goulart, Bioorg. Med. Chem. 20 (2012) 3533–3539.
[25] L.G.S. Brooker, G.H. Keyes, K.H. Sprague, R.H. Vandyke, E. Vanlare, G. Vanzandt, F.L. White, J. Am. Chem. Soc. 73 (1951) 5326–5332.
[26] (a) S. Miyamoto, Chem-Bio Inf. J. 2 (2002) 74–85;
(b) M. Zentgraf, H. Steuber, C. Koch, C.L. Motta, S. Sartini, C.A. Sotriffer, G. Klebe, Angew. Chem. Int. Ed. 46 (2007) 3575–3578;
(c) Z. Wang, B. Ling, R. Zhang, Y. Liu, J. Phys. Chem. B 112 (2008) 10033–10040;
(d) S. Sugunadevi, T. Sundarapandian, K.W. Lee, J. Mol. Model. 18 (2012) 3267–3282;
(e) X. Zheng, L. Zhang, W. Chen, Y. Chen, W. Xie, X. Hu, ChemMedChem 7 (2012) 1921–1923;
(f) V. Shailesh, J. Kamlendra, S. Bhadoriya, S.B. Bari, Med. Chem. Res. 21 (2012) 1665–1676.
[27] M.J. Frisch, G.W. Trucks, H.B. Schlegel, G.E. Scuseria, M.A. Robb, J.R. Cheeseman, G. Scalmani, V. Barone, B. Mennucci, G.A. Petersson, H. Nakatsuji, M. Caricato, X. Li, H.P. Hratchian, A.F. Izmaylov, J. Bloino, G. Zheng, J.L. Sonnenberg, M. Hada, M. Ehara, K. Toyota, R. Fukuda, J. Hasegawa, M. Ishida, T. Nakajima, Y. Honda, O. Kitao, H. Nakai, T. Vreven, J.A. Montgomery Jr., J.E. Peralta, F. Ogliaro, M. Bearpark, J.J. Heyd, E. Brothers, K.N. Kudin, V.N. Staroverov, R. Kobayashi, J. Normand, K. Raghavachari, A. Rendell, J.C. Burant, S.S. Iyengar, J. Tomasi, M. Cossi, N. Rega, N.J. Millam, M. Klene, J.E. Knox, J.B. Cross, V. Bakken, C. Adamo, J. Jaramillo, R. Gomperts, R.E. Stratmann, O. Yazyev, A.J. Austin, R. Cammi, C. Pomelli, J.W. Ochterski, R.L. Martin, K. Morokuma, V.G. Zakrzewski, G.A. Voth, P. Salvador, J.J. Dannenberg, S. Dapprich, A.D. Daniels, O. Farkas, J.B. Foresman, J.V. Ortiz, J. Cioslowski, D.J. Fox, Gaussian 09, Revision B.01, Gaussian, Inc., Wallingford, CT, 2010.
[28] www.biosolveit.de.
[29] H. Haraguchi, R. Hayashi, T. Ishizu, A. Yagl, Planta Med. 69 (2003) 853–855.
[30] M. Jung, H.C. Lee, C.W. Ahn, W. Park, S. Choi, H. Kim, D. Cho, G.T. Lee, H.R. Li, Chem. Pharm. Bull. 50 (2002) 1135–1136.
[31] J.H. Kinoshita, Invest. Ophthalmol. 4 (1965) 786–799.
[32] SMART & SAINT. Software Reference Manuals. Versions 6.28a & 5.625, Bruker Analytical X-ray Systems Inc, Madison, Wisconsin, U.S.A, 2001.
[33] G.M. Sheldrick, SHELXS97 and SHELXL97, Programs for Crystal Structure Solution and Refinement, University of Gottingen, Germany, 1997.